Advanced Drug Delivery Reviews 186 (2022) 114326

Contents lists available at ScienceDirect

Advanced Drug Delivery Reviews

journal homepage: www.elsevier.com/locate/adr

Biodistribution, pharmacokinetics and excretion studies of intravenously injected nanoparticles and extracellular vesicles: Possibilities and challenges ☆

Tore Skotland [a,*], Tore Geir Iversen [a], Alicia Llorente [a,b], Kirsten Sandvig [a,c]

[a] Department of Molecular Cell Biology, Institute for Cancer Research, Oslo University Hospital, The Norwegian Radium Hospital, 0379 Oslo, Norway
[b] Department for Mechanical, Electronics and Chemical Engineering, Oslo Metropolitan University, 0167 Oslo, Norway
[c] Department of Biosciences, University of Oslo, 0316 Oslo, Norway

ARTICLE INFO

Article history:
Received 24 February 2022
Revised 25 April 2022
Accepted 5 May 2022
Available online 16 May 2022

Keywords:
Biodegradable
Cancer therapy
Fluorescent labelling
Microscopy
Nanomedicine
Imaging
Radioactive labelling
Regulatory approval

ABSTRACT

There is a large interest in developing nanoparticles and extracellular vesicles for delivery of therapeutics or imaging agents. Regulatory approval of such products requires knowledge about their biodistribution, metabolism and excretion. We here discuss possibilities and challenges of methods used for such studies, which most often are performed after labelling with radioactive isotopes or fluorescent molecules. It is important to evaluate if the labelled and unlabeled products can be expected to behave similarly in the body. Furthermore, one needs to critically consider whether the labels are still associated with the product at the time of analyses. We discuss advantages and disadvantages of different imaging modalities such as PET, SPECT, MRI, CT, ultrasound and optical imaging for whole-body biodistribution, and describe how to estimate the amount of labelled product in harvested organs and tissue. Microscopy of cells and tissues and various mass spectrometry methods are also discussed in this review.

Contents

Abbreviations: ADME, administration, distribution, metabolism and excretion; CLEM, correlative light-electron microscopy; CT, computer tomography; CyTOF, (mass) cytometry by time of flight; EPR, enhanced permeability and retention; EVs, extracellular vesicles; FDA, Food and Drug Administration; ICP-MS, inductively coupled plasma mass spectrometry; i.v., intravenous; IVIS, In vivo imaging system; LC-MS, liquid chromatography mass spectrometry; LNPs, lipid nanoparticles; LSEC, liver sinusoidal endothelial cells; MR, magnetic resonance; MRI, magnetic resonance imaging; MRS, magnetic resonance spectroscopy; MS, mass spectrometry; MSI, mass spectrometry imaging; NIR, near-infrared; NLCs, nanostructured lipid carriers; NPs, nanoparticles; PDX, patient derived xenograft; PEG, polyethylene glycol; PET, positron emission tomography; PK, pharmacokinetics; PS, phosphatidylserine; SLNs, solid lipid nanoparticles; QDs, quantum dots; QWBA, quantitative whole-body autoradiography; SPECT, single photon emission computed tomography; TEM, transmission electron microscopy.

☆ This review is part of the Advanced Drug Delivery Reviews theme issue on "In vivo fate and cellular".

* Corresponding author.
E-mail address: toresko@uio.no (T. Skotland).

https://doi.org/10.1016/j.addr.2022.114326
0169-409X/

1. Introduction

1.1. Development of nanomedicine

There is currently a huge interest in developing nanoparticles (NPs) and extracellular vesicles (EVs) for delivery of therapeutics and diagnostics for several diseases. There are several definitions of NPs in the literature. For the purpose of this review, we here define NPs as man-made particles, normally consisting of relatively few different substances and with a diameter below 300 nm. In contrast, EVs are produced by cells and isolated from biological materials. They consist of a biological membrane surrounding a water phase and contain several thousand different molecules. Although some EV populations have a size range similar to that of NPs, there is also several EV populations considerably larger than 300 nm. Further description regarding various types of NPs and EVs is provided in Sections 1.2-1.4. There are so far no specific guidelines from the US Food and Drug Administration (FDA) concerning requirements for approval of such products for human use. FDA has not adopted a regulatory definition of nanotechnology but concluded that these products will be approved using the same tools as for approval of other products, i.e. by evaluating their predicted benefit and risk profile [1,2]. All new drug products for human use have to pass a long list of efficacy and safety studies in animals before being tested in humans [3]. This includes Administration, Biodistribution, Metabolism and Excretion (ADME) and pharmacokinetics (PK) studies, which are essential to decide for how long safety studies have to be performed. Non-biodegradable substances may accumulate in the body longer than biodegradable ones and can therefore, as stated in the guidelines for industry, "produce effects related to chronic exposure of the components" [3]. Thus, the toxicity studies for non-biodegradable substances have to last longer than for the biodegradable ones, and the cost of development then increases. FDA has found it necessary to publish a safety notification stating that approval requirements are needed also for products based on EVs [4]. There are many similar considerations to be made when studying ADME or PK of NPs and EVs. A large number of articles has been published in this field (Table 1) and our intention with this article is not to summarize the data reported, but to focus on the opportunities and challenges scientists face when performing such studies following intravenous (i.v.) administration of NPs or EVs. Thus, we aim at providing a qualitative discussion instead of presenting data obtained with different types of NPs. At the end of this review we shortly mention some aspects related to the use of various animal species and animal models in drug delivery studies, and we have also added some considerations about future perspectives, including the usefulness of NPs and EVs for imaging and therapy.

1.2. NPs: Background

A large variety of NPs have been developed. NPs can be made from e.g. lipids, polymers, or inorganic substances such as iron oxide, gold or silica; see [5] for an overview of various types of NPs and also a list of FDA approved nanomedicines. Lipid-based NPs includes liposomes (the most studied lipid-based NPs) and many other particles referred to as lipid nanoparticles (LNPs) [5], solid lipid nanoparticles (SLNs) and nanostructured lipid carriers (NLCs) [6]. Also, the RNA-based COVID-19 vaccines are lipid-containing NPs [7]. Liposomes are the most studied lipid-based NPs and show some similarities to the EVs in having a lipid mem-

Table 1
Number of references found in PubMed searches for "Nanoparticles" or "Extracellular vesicles" alone or in combination with the words given in the left column; searches performed February 21st, 2022.

Search terms	Nanoparticles (NPs)	Extracellular vesicles (EVs)
NPs/EVs	275 000	31 000
NPs/EVs AND degradation	88 000	21 000
NPs/EVs AND biodistribution	4 767	158
NPs/EVs AND excretion	1 105	186

brane surrounding a water phase. In principle, hydrophilic substances can be added to the water phase of both liposomes and EVs. The first liposome-based product for cancer treatment was Doxil®/Caelyx® which contains doxorubicin in the water phase [8]. Liposomes and EVs may also contain lipophilic substances in their membrane, although we are aware of only one such product that has reached the market (AmBisome®) [9]. Similarities and differences between liposomes and EVs and their use as drug delivery systems, including comparison of composition and PK, have recently been discussed [10,11].

Polymeric NPs can be synthesized both from natural or synthetic materials, monomers as well as polymers, thus making it possible to produce a wide variety of structures [5,12]. Drugs or imaging agents can be entrapped in the polymer, conjugated to the polymer and bound to the surface of the NPs, enabling the possibility to carry both hydrophobic and hydrophilic substances. Of the many types of inorganic or metal-based NPs, it is to our knowledge only iron oxide NPs that clearly have been shown to be biodegradable [13,14] and also approved for clinical use [15]. Gold NPs are easy to produce, but they have not been reported to be degradable or are degraded/excreted very slowly. Nevertheless, these NPs have, partly due to their uniform size and detectability, been found very useful for many basic in vitro and *in vivo* preclinical studies, including biodistribution studies in small animals (see Section 2). Also the so-called quantum dots (QDs), which are made of a combination of various metals, have been useful for imaging studies in cells and small animals, but all QDs made so far are to our knowledge not degradable and too toxic to be approved for human use [16]. In contrast to the other particles discussed above, solid metal-based NPs can only carry drugs or other substances on their surface. In the case of mesoporous silica NPs, the substances may also be bound inside the pores.

1.3. EVs: Background

There are several types of EVs released by cells. Such vesicles can originate either from structures inside the cells or from the plasma membrane. Most EVs studied have so far been performed with EVs defined as exosomes by the authors. Exosomes are vesicles with a size of 40–150 nm (i.e. a size range similar to most NPs studied for drug delivery), released by fusion of multivesicular bodies with the plasma membrane. Thus, exosomes correspond to the intraluminal vesicles found inside the multivesicular bodies that fuse with the plasma membrane [17]. There are also several reports demonstrating that various intracellular organelles can be excreted via secretory autophagy [17], and one report describes such EVs to be smaller and have an inverted membrane topology compared to exosomes [18]. EV release from the plasma membrane can be induced by various cell death processes such as apoptosis and necroptosis and even processes occurring with the purpose of rescuing cells from cell death; reviewed in [19,20]. As discussed in these reviews, most of such EVs are larger than exosomes and have phosphatidylserine (PS) in the outer leaflet as an "eat me" signal for macrophages. In this article we will not discriminate between exosomes and other types of EVs and thus not focus on how these biological EVs are produced by cells. It should, however, be noted that it is likely that EV populations will be circulating for a shorter time if having PS present in the outer leaflet. A list of different types of EVs are given in Table 1 in [21]. Labelling of different mixtures of these EVs or samples containing various lipoproteins [17] may thus result in different outcome of PK or ADME studies. For general information about the biology, biomedical applications and overviews of preclinical and clinical studies with EVs, we refer to the following recent review articles [22–25].

1.4. NPs versus EVs: Initial considerations

There are several important differences between EVs and NPs. One is that EVs are composed of a huge number of different molecules; their surrounding membranes contain hundreds of different lipid species and membrane-bound proteins, and the lumen of these EVs contains a large number of proteins, nucleic acids, lipids, amino acids and other metabolites. Thus, a major effort is required to characterize the molecular composition of EVs and demonstrate the reproducibility between batches, as needed to bring such products into clinical use. We have earlier shortly discussed this issue [26] and the studies needed to bring NPs into clinical use [27]. Those aspects will therefore not be discussed here. Neither will we discuss toxicity issues related to NPs or EVs, except for mentioning that there are several lines of evidence that *i.v.* injection of EVs may be very well tolerated. Thus, blood transfusions have been safely carried out for more than 50 years, and blood is now known to contain large amounts of EVs. Also, EVs of mouse or human origin did not give severe immune reactions when administered repeatedly in mice [23].

As discussed below many types of labels can be used to visualize and/or quantify the amounts of NPs or EVs or their constituents in whole animals, tissue samples or other biological material such as blood, urine and feces. It is important to be aware of that attaching labels on the surface of NPs or EVs may change their surface properties and result in a different biodistribution than that of the unlabeled particles. Thus, the size distribution and zeta potential before and after labeling should be compared, but there may also be important changes in surface properties that are difficult to detect. One should especially be careful when interpreting data obtained following addition of hydrophobic labels (e.g. fluorescent molecules) on the surface of NPs and EVs. If covalently bound, the fluorescent label may significantly change the surface properties, and if noncovalently attached dye leakage may occur. In the draft guidelines for industry mentioned above it is clearly stated that "Data should be collected demonstrating that the label does not substantially affect the biodistribution of the nanomaterial" [2].

Another issue to keep in mind when coupling molecules to proteins, which often is done via lysine (pKa $\sim$ 10.5), is that such covalent modifications not only add a new structure on the surface, but it also removes a positive charge from the surface. The importance of changing surface properties such as the charge of EVs was clearly demonstrated by the major changes observed in biodistribution of EVs following treatment with neuraminidase, which removes terminal negatively charged sialic acid from glycoproteins [28].

When interpreting biodistribution data it is important to consider if the label is still bound to the NPs or EVs at the time of analysis. Has the label been split from the particles or has the radioactive metal been separated from the chelator it was bound to? More details of such issues are discussed below. We will here just mention that NPs larger than 10 nm are not excreted to any significant amount in urine (further discussed in the next section). Thus, detection of radioactivity in urine following *i.v.* injection of radioactively labelled NPs larger than 10 nm, is either due to a very minor fraction of the injected NPs being excreted in urine or to the excretion of the radiolabel or a degradation product containing the radiolabel.

2. Circulation of NPs and EVs and possibilities to exit from blood

Most EVs and NPs studied have a diameter in the size range of 30–200 nm, whereas some NPs such as QDs and gold NPs can be much smaller with a hydrodynamic diameter of just a few nm. The gaps between endothelial cells are normally less than 2 nm,

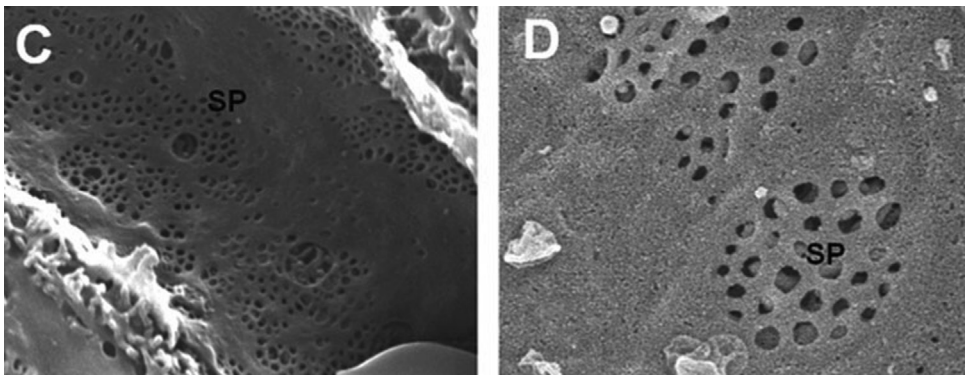

Fig. 1. Scanning electron micrographs showing the fenestrated wall of the sinusoidal endothelium of rat liver. These images are copied from Le Couteur *et al.* [31] (Fig. 1C and D in that article). C: Luminal surface with fenestrae of approx. 50–150 nm forming clusters called sieve plates (SP). D: Higher magnification of one sieve plate with many fenestrae. Reproduced with approval from John Wiley and Sons.

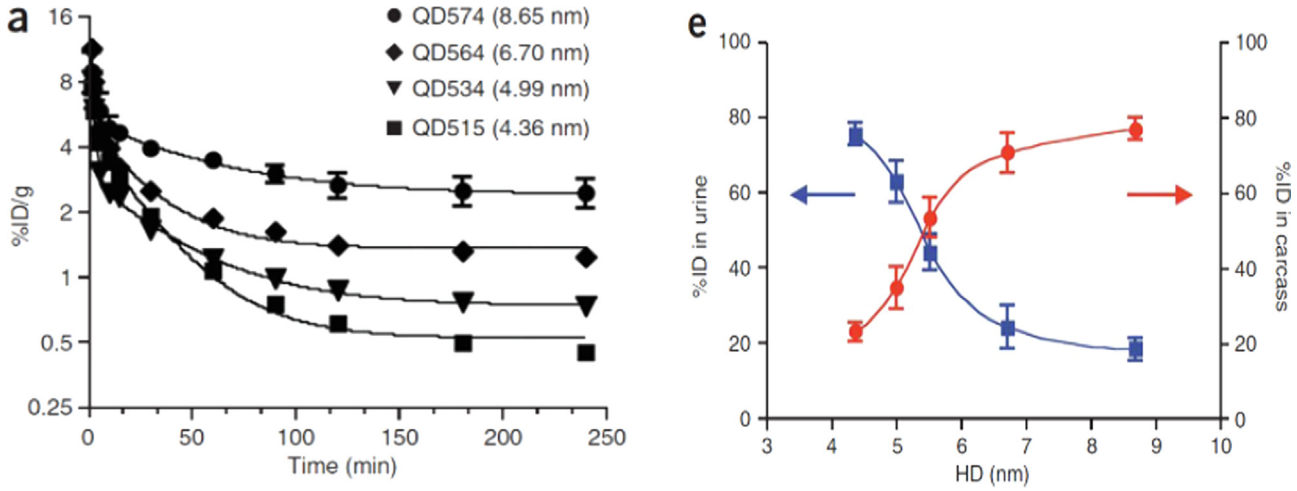

Fig. 2. Blood clearance and percent of injected dose of QDs recovered in urine and carcass. These figures are copied from Choi *et al.* [42] (Fig. 3a and 3e in that article). **a.** Blood concentration shown as percent of injected dose per g (%ID/g) following *i.v.* injection in mice of QDs with the hydrodynamic diameters (HD) shown in parentheses. **e.** Urine excretion (blue curve) and carcass retention (red curve) of the QDs 4 h after i.v. injection (mean ± SD; 5 animals). Reprinted by permission from Springer Nature. (For interpretation of the references to colour in this figure legend, the reader is referred to the web version of this article.)

which restrict the ability of most NPs to exit blood following *i.v.* injection. The NPs may, however, pass through fenestrae (small holes) with a diameter up to 200 nm in the endothelium of liver (Fig. 1), spleen and bone marrow; kidneys have fenestrae of 20–30 nm, whereas other tissues have very small (diameter less than 6 nm) or no fenestrae [29–32]. Importantly, there is a leakier endothelium in inflammation areas and in solid tumors where the NPs may exit from blood. The most effective way for NPs to reach tumors following *i.v.* administration has for many years been regarded to be passive enrichment in tumors due to the so-called Enhanced Permeability and Retention (EPR) effect [33,34]. Thus, the accumulation is caused by the combination of an increased extravasation (enhanced permeability) and a decreased drainage by the lymphoid system (increased retention). It was recently proposed that NPs reached tumors by an active transport across the endothelial cell layer [35], but as discussed we do not think this has been convincingly demonstrated and more studies are needed to clarify how most NPs pass the endothelial cell layer and enter tumor tissue [36].

A very small amount of the injected dose of NPs ends up in the tumors. In a meta-analysis with data from more than hundred preclinical studies, it was calculated that only 0.7% (mean value) of the *i.v.* injected dose reached the tumor [37]. Although there is no doubt that a very small amount of the injected dose reaches the tumors, several authors have discussed that this percentage is uncertain and may be too small. Importantly, in order to evaluate the usefulness of NPs, one needs to consider several other issues than just how much of the NPs that ends up in the tumors [38,39]. Furthermore, it was reported more than 20 years ago that injecting soluble targeting molecules (e.g. antibodies) for tumor therapy or imaging resulted in much less than 1% of the injected dose being retained per gram tumor in humans [40]. Thus, by conjugating targeting molecules to NPs one should not expect a significant increase in the amounts of NPs or drugs ending up in tumor tissue. However, such targeting molecules may still be important for uptake into cells and thus improve the therapeutic effect. If addition of targeting molecules to NPs significantly change their biodistribution, one should consider if this may be due to changes in surface charge or hydrophobicity. Furthermore, based on the low fraction of injected NPs that ends up in tumors, one should not expect to see significant different biodistributions in small animals whether they are tumor-bearing or not.

Small NPs can be excreted through kidneys if being small enough to pass through the kidney filtration units called glomeruli [41]. It is now almost 15 years since the publication of the seminal study by Choi *et al.* [42], where they demonstrated glomerular filtration and rapid renal excretion in mice of approx. 50% of the injected dose of NPs with a hydrodynamic diameter of 5 nm,

whereas there was less than 20% excretion of 9 nm NPs (Fig. 2). Since most NPs used for drug delivery are larger than 10 nm, it is very important, both for safety issues and for formal regulatory aspects, that the NPs are degradable and thus hopefully excreted. This is not a problem with EVs or for NPs made of endogenous substances, like liposomes or albumin-based NPs. It is probably also not a problem with iron oxide-based NPs, as such superparamagnetic particles are biodegradable and have been safely used as contrast agents for magnetic resonance imaging (MRI) for more than 20 years [15]. However, there are in fact very few data demonstrating degradation and excretion of most other NPs.

NPs just slightly larger than the NPs used in the excretion studies by Choi *et al.* [42] seem to end up in the liver. Iron oxide NPs with a hydrodynamic diameter of 12 nm were mainly taken up by liver, in approximately similar amounts by Kupffer cells and liver sinusoidal endothelial cells (LSEC) [14]. Lipodisq NPs with a hydrodynamic diameter of 10 nm were also mainly taken up by liver and rapidly excreted in feces so more labelled substance was found present in feces within colon than in kidneys 4 h after injection [43]. There are a few reports describing that some NPs considerable larger than 10 nm were able to bypass the glomerular filtration barrier and end up in urine. We refer to a recent article by Adhipandito *et al.* who reviewed this phenomenon and speculated about mechanisms involved [44].

Two biodistribution studies performed almost 25 years ago nicely illustrate what may happen following *i.v.* injection of gold NPs with different sizes. One study was performed using gold NPs of 15, 50, 100 and 200 nm in mice and the other was performed with gold NPs of 10, 50, 100 and 250 nm in rats. The largest NPs were in both studies mainly taken up by liver and spleen, whereas the smallest NPs were present in most tissues [45,46]. The smallest NPs, which are not rapidly taken up liver/spleen, will circulate for a longer time and can thus be endocytosed by different cells. The rate of endocytosis differs between cell types and can be very fast for some cells. Thus, macrophages ingest 25% of their own volume every hour, whereas fibroblasts endocytose at approximately one third the rate of macrophages [47]. We refer to the following review articles regarding discussions of the expected biodistribution, excretion and PK of various NPs following *i.v.* injection [48–50]; one of these nicely illustrates how the circulation time increases with decreasing hydrodynamic diameter of metal-based NPs with polyethylene glycol (PEG) [50]. It should be noted that whereas it is the size of the metal core that determine the MRI signal intensity for iron oxide NPs, it is the hydrodynamic diameter that is important regarding circulation half-life and penetration into tissue. Thus, the length of e.g. PEG chains added to increase the circulation time in blood is important also for tissue penetration. Based on these considerations and the knowledge about cellular uptake of NPs [51], it is likely that the optimal size of NPs for drug delivery is in the range 20–200 nm.

Injecting substances that are excreted rapidly in urine may be beneficial for imaging as it is important to reduce the signal from the surrounding tissue to better visualize a diseased area. Thus, most contrast agents used in the clinic are low molecular weight substances that are almost completely excreted in urine within 24 h post dosing. One can often see authors stating that it may be beneficial to inject very small NPs that are rapidly excreted in urine in order to reduce toxic effects. But what is the benefit of using NPs if they are rapidly excreted in urine? NPs are more complex to produce, and more studies are needed to obtain the necessary safety and efficacy data required to obtain approval for clinical use compared to the traditional low molecular weight contrast agents.

For NPs bearing drugs to have a therapeutic effect, it will be an advantage to have the NPs circulating for a longer time in order to get as much drug as possible to the diseased area. Also, a prolonged exposure to the drug after injection is likely to increase the therapeutic effect. Certainly, more knowledge about the interaction between NPs and EVs and the animal/human body is required to bring more of these products into clinical use.

At the end of this paragraph we would like to remind the reader that our comments are related to what can be expected following *i.v.* administration. Other routes of injection will result in a different biodistribution and pharmacokinetics and will not be discussed in this article. We would, however, like to stress that it has been shown that even injection of ultrasound contrast agents with a mean size of 3 μm into breast tumors, makes it possible to detect metastases in sentinel lymph nodes due to a passive diffusion of these microparticles [52].

3. Biodistribution studies using imaging methods

3.1. Different imaging modalities, their properties, sensitivities and depth of imaging

Many different imaging modalities used in the clinic can also be applied when studying biodistribution in small animals. Some key properties of positron emission tomography (PET), single photon emission computed tomography (SPECT), magnetic resonance imaging (MRI), computed tomography (CT), optical/fluorescence imaging and ultrasound imaging are shown in Table 2, which includes information about the spatial resolution, limit for depth

Table 2
Some characteristics of imaging modalities and contrast agents used in the clinic.

Imaging modality	Spatial resolution	Limit for depth of imaging	Sensitivity (M: mol/L)	Agents/probes that can be used for the modality	Amount of agent injected in humans
PET	1–2 mm	No	$10^{-11} - 10^{-12}$ M	Radiolabel (positron emitters, e.g. ^{18}F, ^{11}C, ^{13}N, ^{62}Cu,^{68}Ga,^{124}I)	Nanograms
SPECT	1–2 mm	No	$10^{-10} - 10^{-11}$ M	Radiolabel (gamma emitters, e.g. ^{99m}Tc, ^{111}In, ^{123}I, ^{125}I, ^{131}I, ^{201}Tl)	Micrograms
Optical/ Fluorescence[1]	~ 1/10 of depth of imaging	From less than 1 cm and up to 10 cm	$10^{-9} - 10^{-11}$ M	Fluorescent molecules	Micrograms to milligrams
Ultrasound	50–500 μm	No?[2]	See footnote[3]	Gas-filled microbubbles	Micrograms to milligrams
MRI	25–100 μm	No	$10^{-3} - 10^{-5}$ M[4]	Paramagnetic metals or ferromagnetic particles	Milligrams to grams
CT	50–200 μm	No	$10^{-2} - 10^{-3}$ M	Iodine-containing molecules. Other heavy atoms can be used.	Grams

[1] Large differences in the parameters listed due to a variety of optical methods. Depth of imaging less than 1 cm for reflectance imaging; up to approx. 10 cm with fluorescence tomographic technique.
[2] Reduced signals from deep tissues, depending upon the frequency used.
[3] Depends very much on bubble size and structure, and the frequency used; single bubbles may be detected.
[4] Cells labeled with iron-oxide NPs may be detected with a sensitivity close to that of SPECT.

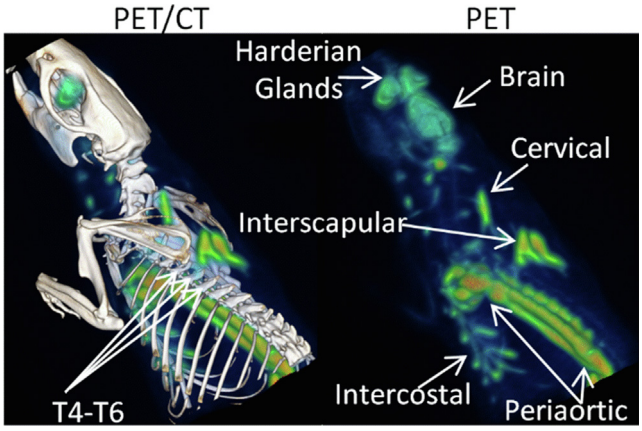

Fig. 3. Example of a PET-CT image of mice. The PET image is obtained using ^{18}F-FDG uptake in beta3-adrenergic receptor agonist-activated brown adipose tissue. Image reproduced from Fig. 4C in an open access publication by the group of Jogeshwar Mukherjee [58].

of imaging, sensitivity and agents/probes used as contrast agents for the various modalities [53]. CT, MRI, SPECT and PET are often used for whole body imaging and it has been estimated that the numbers of procedures performed with these modalities per year in USA are 80, 40, 6 and 2 million, respectively (these numbers are estimates based on information obtained from several Web resources). More information regarding the specificity, user-friendliness and some advantages and disadvantages of using the various imaging modalities for studies of small animals are further discussed in Section 3.2.

3.2. Whole body imaging in small animals

3.2.1. PET and SPECT

The two nuclear medicine imaging modalities PET and SPECT are commonly used in the clinic for imaging of different diseases and they are also useful for imaging of small animals like mice (then normally using equipment called micro-PET and micro-SPECT). These techniques can be used to obtain three-dimensional quantitative images of the radioactive tracer injected, and signals can be acquired as a function of time.

PET imaging is based on detection and quantification of positron emitters; ^{18}F is by far the most used isotope for such imaging (mainly as [^{18}F]fluorodeoxyglucose imaging of cancer), but also other isotopes as those listed in Table 2 may be used [54–56]. Although PET imaging is an excellent technique to obtain good and quantitative images, this modality is not straight forward to use in research laboratories because a cyclotron is needed to produce the positron emitters, which also have the draw-back of having very short half-lives (110 min for ^{18}F; shorter for the other PET tracers listed in Table 2). PET imaging is extremely sensitive, but PET cannot detect exactly where in the body the emitters are localized. Thus, it is often necessary to use dual imaging by combining PET with either CT or MRI. When using PET-CT or PET-MRI, PET delivers the sensitive detection of the emitters and CT or MRI give an excellent anatomical map of the body and thus shows where the emitters are localized [57]. An example of a PET-CT image of mice (from [58]) is shown in Fig. 3.

SPECT imaging is based on detection of gamma emitters. The most commonly used isotopes for SPECT are shown in Table 1; ^{99m}Tc is the most used isotope for this imaging modality. This is because ^{99m}Tc has a favorable energy, a short half-life of 6 h, and is easily available in almost all clinical imaging facilities worldwide. This availability is due to that ^{99m}Tc is a daughter product of ^{99}Mo (half-life of 67 h) which can be delivered on columns called ^{99}Mo/^{99m}Tc generators [59,60]. Thus, by supplying the laboratories once per week with such ^{99}Mo/^{99m}Tc-containing columns, researchers can elute ^{99m}Tc from the column when they need this isotope just by adding saline to the column; see [61]. As described above for PET, it is also very useful to combine SPECT with MRI or CT. Recently, Uenomachi *et al.* published a new method that allows similar *in vivo* imaging with PET and SPECT tracers using a Compton-PET hybrid camera [62].

3.2.2. MRI and CT

MRI and CT can be used to obtain very detailed anatomical and functional images in patients and are also useful for studies of small animals. MR techniques are based on detecting radiofrequency signals generated by the nuclear spin of MR active nuclei such as ^{1}H, ^{13}C, ^{19}F and ^{31}P. Thus, MRI was originally called nuclear magnetic resonance imaging, but nuclear was dropped to avoid negative associations with radioactivity. Most MR images are obtained by benefiting from the nuclear properties of protons in low molecular weight substances that are free to move around, i.e. mostly water, lipids (not membrane-associated lipids) and other metabolites. Contrast agents for MRI have been available in the clinic for more than 30 years. By far the most commonly used of such contrast agents are low molecular substances where the paramagnetic metal Gd^{3+} is bound to a chelate. Also, other paramagnetic metals such as Mn^{2+} may be used to change the so-called T1- weighted images (making the image brighter) close to these contrast agents. Superparamagnetic or ferromagnetic particles (e.g. iron-oxide-based NPs) may similarly be used to affect the T2-weighted images (making the image darker); for a review of the principles of MRI and the contrast agents used, see [63]. Magnetic NPs can also be imaged using a quantitative tomographic technique called magnetic particle imaging or MPI [64].

Of the contrast agents used in the clinic, iron-oxide based NPs are the most commonly used in preclinical studies as imaging agents or for delivery of therapeutics. One can read in many review articles that all iron-oxide NPs earlier used as contrast agents for MRI now have been removed from the marked due to safety reasons; see e.g. [65]. However, as discussed by Dadfar *et al.* [66], there are reasons to believe that at least some of these iron oxide-based products were removed from the marked due to commercial reasons. One of the authors of this article (Skotland) was involved in industrial development of another agent than those discussed by Dadfar *et al.* and knows that development of also NC100150 (Clariscan, Nycomed) was stopped because of commercial reasons, and not because of safety issues. Thus, we agree with Dadfar *et al.* [66] that iron-oxide NPs should be further evaluated for human use. This view also fits with the fact that there are several iron-based nanomedicines that are approved and found safe to inject in persons with iron deficiencies [5]. It should also be noted that one of the products used to treat iron deficiency has been reported to inhibit tumor growth by inducing pro-inflammatory (anti-tumorigenic) macrophage polarization in tumor tissue [67]. Notably, publications containing high quality pharmacokinetic, biodistribution and toxicity studies have been reported for the iron-oxide based NPs approved for clinical use; reviewed in [68].

CT is based on the use of X-rays and is together with MRI the most used imaging modalities in radiology. Both methods can give very high-quality three-dimensional anatomical images and are also very useful for imaging of small animals. Almost all contrast agents approved during the last 60 years for X-ray-based techniques, including CT, have a high content of iodine (tri-iodinated benzene rings), although in principle also other heavy atoms can be used [69]. Injection of these contrast agents helps in visualizing blood vessels and identification of many diseases. The use of micro-CT in the absence or presence of contrast agents, either

agents used in the clinic or agents not approved for human use (e.g. gold or other metal-based NPs), can be used to obtain excellent images of mice [69,70].

3.2.3. Ultrasound imaging

Ultrasound imaging has been popular in the clinic for many years. Most people know about the use of ultrasound imaging related to control during pregnancy and functional imaging of the heart, but ultrasound is also very useful for imaging of many other conditions; see [71]. During the last 25 years several contrast agents for this modality have entered the marked and opened up for additional use of ultrasound imaging in the clinic [72]. To benefit from this modality in studies of small animals it is necessary to make specific transducers with other frequencies than those used for patients [73], and ultrasound is less used for imaging of small animals than the modalities discussed above. It should be noted that contrast agents for ultrasound may improve the extravasation of NPs out of blood vessels and thus give a higher accumulation and penetration into cancer tissue. Thus, ultrasound has been proposed to be a good strategy, especially for improving drug delivery to tumor types which show a low EPR effect [74].

3.2.4. Optical imaging

Optical imaging, which is mainly based on using fluorescent substances, is much less used in the clinic than PET, SPECT, MRI, CT and ultrasound imaging. Optical imaging can, however, be very useful for specific analyses in the clinic and it is so far the most used imaging modality for biodistribution studies in small animals. Due to a variety of optical methods, the spatial resolution, penetration into tissue, depth of imaging and sensitivity differ very much between the various optical methods (Table 2). Optical imaging methods based on using fluorescence detection in the 400–700 nm range will due to light scattering, low penetration and tissue autofluorescence result in low imaging sensitivity. However, the use of detection in the first or second near-infrared window, i.e. NIR-1 in the 700–900 nm range or NIR-2 in the 1000–1700 nm range, will result in better penetration and both improved signal-to-background ratios and reduced tissue autofluorescence; reviewed in [75]. Since light is not penetrating well through tissue, both the signal intensity and the spatial resolution become worse for light that has passed through tissue. Thus, optical imaging is most useful in the clinic when the optical agents are present on body surfaces, including areas that can be reached with endoscopes, e.g. the gastrointestinal tract and the bladder [76]. The use of various dyes may also be very useful to guide surgeons during cancer surgery, e.g. to find and remove the sentinel lymph nodes in breast cancer patients [77].

Fluorescence labelling of NPs and EVs seems to be the most popular way to label these particles to study their biodistribution in small animals. Whole body images of such fluorescently labelled particles can be obtained using e.g. IVIS® imaging (In Vivo Imaging System) which also can be integrated with CT. Labelling of NPs and EVs for biodistribution studies in small animals, including opportunities and challenges associated with these methods is further discussed in Section 4.2.

3.3. Imaging of organs/tissues and tissue slices

As shown in Table 2 there is in principle no limit for depth of imaging when using PET, SPECT, MRI or CT, whereas the signal intensity and resolution of optical signals decrease when passing through tissue. Thus, it may be beneficial to perform *ex vivo* imaging on isolated organs from sacrificed animals to obtain stronger fluorescence signals. One draw-back with such end-point analyses is that it only allows one time point for each animal, thus adding the uncertainty of using several animals to obtain data for different time points. Also, when quantifying signals using isolated organs, one must remember that the signal intensity decreases with the depth of the tissue, and that the data therefore should be regarded as semiquantitative, as discussed further in Section 4. It is also important to measure the background fluorescence of similar tissues from animals not injected with the substance as various tissues show a different fluorescence background [78]. For all analyses of isolated organs, one should keep in mind the signals originating from blood within these organs (it is not possible to remove blood from all organs). It should also be mentioned that various tissue optical clearing techniques have recently been developed. The optical clearing is obtained by treating tissue/organs with chemicals to make the tissue transparent, thus facilitat-

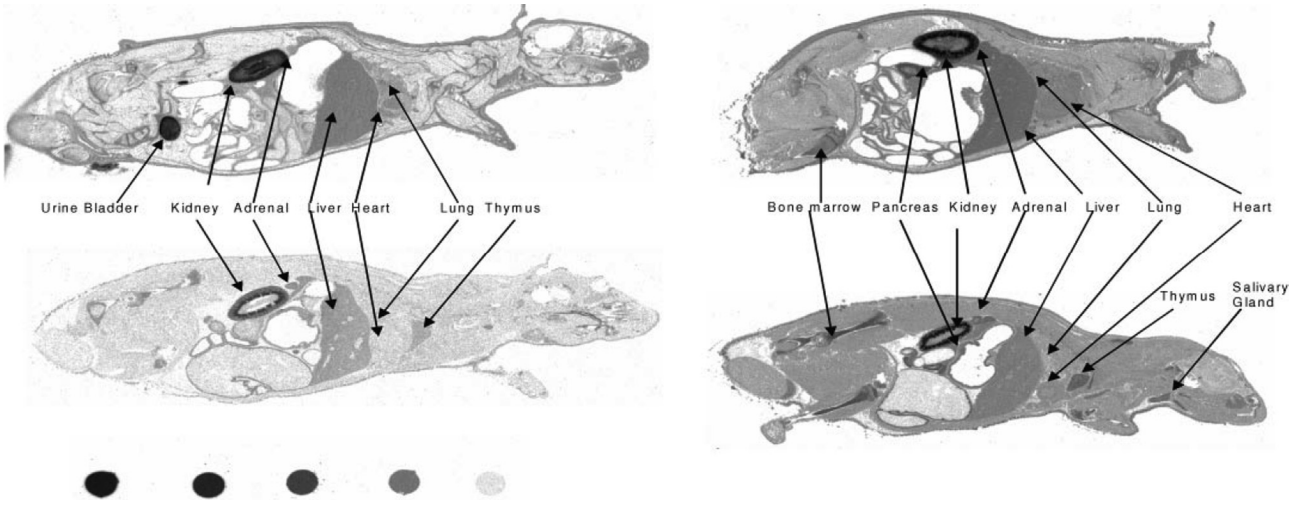

Fig. 4. Illustration of use of QWBA in rats. A peptide with 13 amino acids was studied as a tracer for venous thromboembolism. The peptide was labelled in the N-terminal (Asn-U-^{14}C; the two images to the left) or close to the C-terminal (Lys-U-^{14}C; the two images to the right). Top images taken from animals 20 min post dosing; bottom images taken 24 h post dosing. The images were obtained using cryosections with a thickness of 25 μm. These images combined with LC-MS analyses demonstrated how the peptide was metabolized. The N-terminal part was excreted in urine, whereas the Lys close to the C-terminal was to a major extent incorporated into protein metabolism. For further information see [80] from where this figure was copied (Fig. 2 in that article); copied with approval from The American Society for Pharmacology and Experimental Therapeutics.

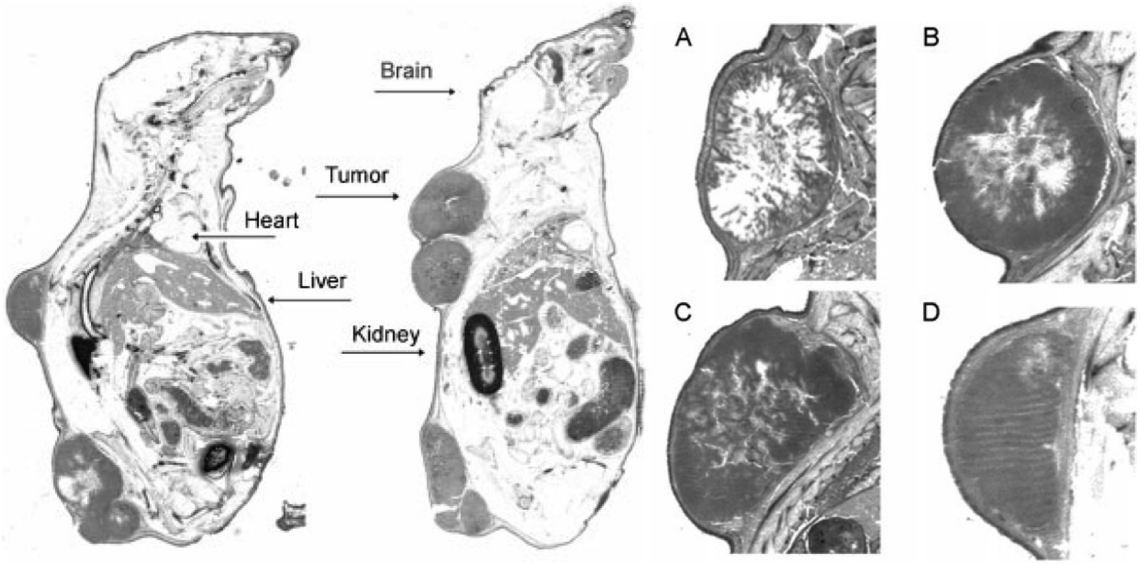

Fig. 5. Illustration of the use of whole-body cryosection fluorescence imaging of mice. A peptide intended to be used for colorectal cancer imaging was labelled with the fluorophore Cy5; for further details see [78] from where these images are copied. The whole-body images to the left were obtained 120 and 240 min after dosing (part of Fig. 3 in the article). The enlarged images of the tumor to the right were taken 5 min (A), 30 min (B), 60 min (C) and 120 min (D) post dosing (part of Fig. 4 in the article). Images were obtained using cryosections with a thickness of 75 μm. Figures reproduced with approval from John Wiley and Sons.

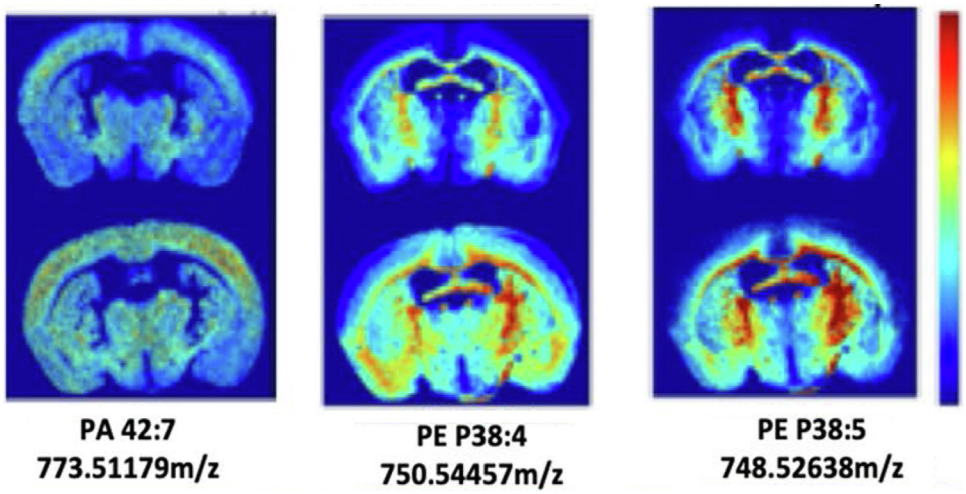

Fig. 6. Illustration of mass spectrometry imaging of mice brain. The images are generated from *m*/*z* signals that were found significantly different in the striatum region of obese mice compared to control mice (top images after feeding with high fat diet for 16 weeks; lower images after feeding for 23 weeks). The *m*/*z* signals for the masses shown represent three different lipid species as shown below the images. Images are shown for obese mice only, just to illustrate the resolution one can expect to obtain with this technology today. The sections have a thickness of 12 μm. For further details see the open access article by Sighinolfi *et al.* [85] from where this figure is copied (their Fig. 7F).

ing imaging deeper into the tissue while preserving spatial resolution; reviewed in [79].

The possibility to make thin slices of tissue (thickness often in the range 20–100 μm) and obtain very detailed whole-body images of such tissues using radioactive isotopes have been exploited for many years. The whole-body autoradiography images obtained may be overlaid photographical images of the tissue slice to determine the localization of the isotopes. By quantification of the signal intensities from the radioisotopes one can obtain what is known as quantitative whole-body autoradiography (QWBA). Originally, QWBA was performed using photographic films, but later imaging plates that could detect both radiographic and fluorescent signals were developed and opened up for using whole-body section fluorescent imaging in biodistribution studies of fluorescent signals in small animals. Examples from own research on biodistribution of substances using whole body slices with QWBA of rats [80] and fluorescence detection in mice [78] are shown in Figs. 4 and 5, respectively.

Thin slices of tissues can also be used for other types of imaging; the thickness of slices used for the methods discussed below in this section is often in the range 3–15 μm. One possibility is to use e.g. fluorescently labelled antibodies and immunohistochemistry to detect and quantify specific proteins [81]. This method is mostly used for selective identification of proteins/biomarkers in tissue samples but may also be useful for e.g. identification of cells containing labelled NPs or EVs. Such analyses have until recently been time consuming, including much manual work, but new instruments allowing automatic digital quantification of immunohistochemistry-labelled slides are now available. Regarding the possibility to use NPs or EVs to deliver drugs for anticancer therapy it is of interest to localize and/or quantify the amount of such particles not only in cancer cells in tumors, but also

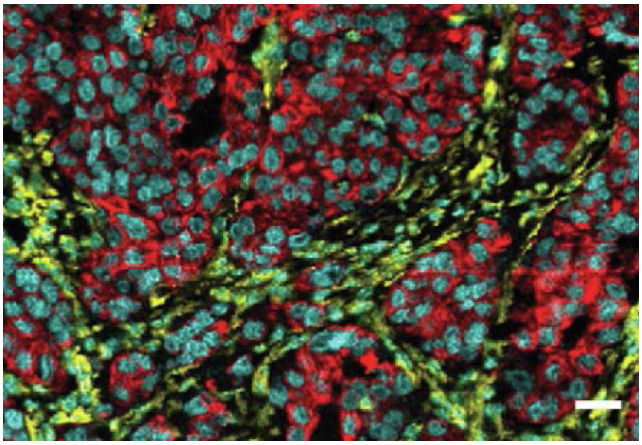

Fig. 7. Image obtained of a tissue sample from a luminal HER2 + breast cancer tissue using high-resolution laser-ablation to CyTOF mass cytometry. This image is copied from the first study using this technology. A total of 32 proteins and phosphorylation sites were measured simultaneously at 1 μm resolution. This image shows cytokeratin (red), histone H3 (cyan) and vimentin (yellow). The section has a thickness of 5 μm; the scale bar is 25 μm. For further details, including information about other proteins imaged, see Giesen *et al.* [89], from where the figure is reprinted (their Fig. 3A) with permission from Springer Nature. (For interpretation of the references to colour in this figure legend, the reader is referred to the web version of this article.)

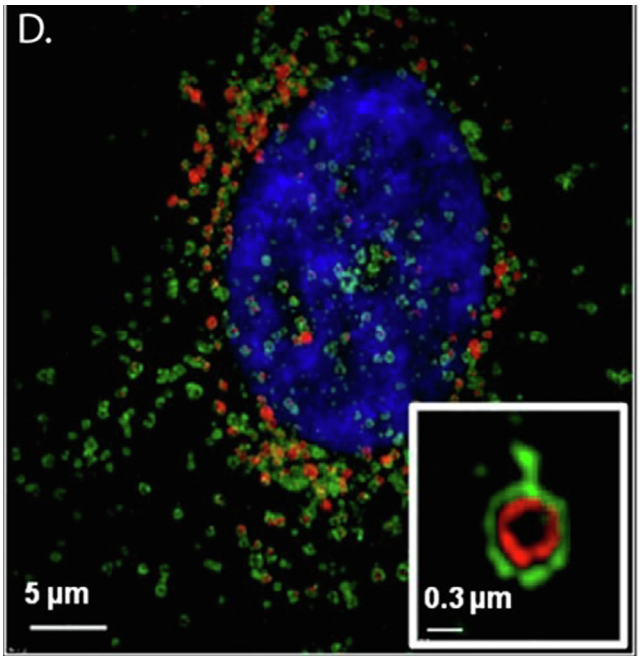

Fig. 8. Structured illumination microscopy image of an MDA-MB-231 cell which has taken up NPs. The NPs are labelled red and the lysosome membrane (LAMP1) is labelled green, thus clearly demonstrating NPs within the lysosomes. For further details see Pandya *et al.* [94] from where this figure is copied (Fig. 8D in that article) with approval from ACS. Further permission related to the material excerpted should be directed to the ACS. (For interpretation of the references to colour in this figure legend, the reader is referred to the web version of this article.)

in cells in the tumor microenvironment such as anti-tumorigenic and pro-inflammatory M1 type macrophages versus the M2 type of macrophages being pro-tumorigenic and anti-inflammatory [82].

It should also be mentioned that newly developed high-resolution microscopy methods have made it possible to analyze localization of fluorescently labelled particles, including cellular uptake, in tissue slides used for immunohistochemistry (for more details see Section 3.4). Furthermore, intravital microscopy, which initially was dependent on very expensive multi-photon microscopes, can now be performed on more conventional imaging platforms such as confocal, spinning disk and epifluorescense microscopes, which provide excellent spatial and temporal resolution 50–100 μm below the surface [83]. In a recent tutorial review Haddad *et al.* discuss sample preparations and microscopy methods to study three-dimensional visualization of archival tissue material [84].

There are several mass spectrometry-based imaging (MSI) techniques that by directly measuring the mass of molecules can provide visualization of molecules present in a tissue slide (Fig. 6; images from [85]). These MSI techniques are all mainly qualitative or semi-quantitative. For further details regarding information about the various MSI techniques including their spatial resolution, mass range detected and analytes we refer to two recent general review articles [86,87] and one review discussing the use of such techniques in pharmaceutical discovery and development [88]. Finally, lanthanide isotopes can be attached to antibodies and used to simultaneously image more than 40 proteins with a subcellular resolution (approx. 1 μm) using laser ablation CyTOF mass cytometry as illustrated in Fig. 7 [89]. These MS-based methods are very resource demanding; it takes time and high expertise to handle such big data analyses.

3.4. Analyses of single cells by flow cytometry and microscopy

Flow cytometry is a valuable tool to sort and analyze cells [90]. Although it has mostly been used to analyze blood cells, it can also be used to analyze cells from tissue samples following mechanical dissociation or enzymatic treatment [91]. Characterization of the various cells in the sample can be performed by using fluorescently labelled antibodies or lanthanide isotopes attached to antibodies [92], i.e. similarly as described above for imaging of tissue slides. Up to at least 40–50 different proteins can be identified using flow cytometry depending on the detection principle. Microscopy has also now for many years been used to study uptake of fluorescently labelled particles into cells. In addition to traditional confocal imaging, newer methods include several high-resolution methods and metal NPs can also be studied by transmission electron microscopy (TEM) and correlative light-electron microscopy (CLEM), a combination of optical microscopy and electron microscopy. Regarding use of different microscopy methods, we refer to Table 3 in [21] which includes information about resolution, illumination method, probes used, acquisition information and whether the methods can be used on live or fixed material. Also, Raman microspectroscopy could be a useful technique for such studies [93]. One example from our own research demonstrating NPs to be present within lysosomes [94] is shown in Fig. 8. By using super-resolution microscopy, Paramasivam *et al.* [95] recently demonstrated localization of single lipid nanocapsules within different endosomal compartments.

4. Labelling of NPs and EVs: Opportunities and challenges

In the previous sections the general properties of the several imaging modalities have been discussed. In this chapter we aim at critically discussing opportunities and challenges by using such methods for biodistribution studies in small animals. Readers interested in getting an overview of the many biodistribution studies performed are referred to the following review articles for NPs [48–50] or EVs [10,96–98]. In short, the studies summarized in these reviews show that EVs in general are cleared much faster from blood than most NPs. Although the biodistribution of various

NPs and EVs differs considerably, these particles have in common that they mainly are taken up by liver, spleen, lungs and kidneys (discussed below).

4.1. Radioactive labelling for PET or SPECT

As detailed in Table 2 and in the articles cited in Section 3.2.1, several isotopes and methods can be used to label NPs and EVs for PET or SPECT imaging. Most of these methods include the binding of the isotopes to a chelate covalently attached to the surface of NPs or EVs. As mentioned above, it is important to consider if addition of such molecules to the surface of the particles may change their biodistribution, and also consider if the added isotope is actually attached to the NPs or EVs at the time of imaging. Such discussions are in fact often missing in the literature.

Liposomes and EVs can be labelled with lipophilic agents that penetrate the lipid membrane and are trapped inside, and this labelling should not significantly change the surface of these particles. Thus, the lumen of these vesicles has been labelled with e.g. ^{111}In-oxine [99], ^{111}In-tropolone [100] and ^{99m}Tc-HMPAO [101,102] for SPECT imaging and with ^{64}Cu chelated to 4-DEAP-ATSC for PET imaging [103]. Examples of labelling on the surface of NPs or EVs include ^{64}Cu bound to NOTA for PET imaging [104] and ^{99m}Tc-tricarbonyl [105,106] or ^{111}In-DTPA [100] labelling of proteins or amino groups for SPECT imaging. Iodine isotopes have also been used for labelling of proteins for many years, and several iodine isotopes can be used for PET [28] and SPECT imaging (Table 2). It should be noted that agents that are used for labelling of proteins in NPs or EVs will also label proteins not associated with these particles in the samples, thus giving rise to signals that are not associated with the particles even at the time of injection. As mentioned in the Introduction, one needs to take into consideration that binding of chelates to proteins often includes binding to lysine, which means that not only is a new structure added, but a positive charge on the surface is removed. For recent reviews discussing labelling of EVs or NPs for PET and SPECT, including other isotopes and chelates than mentioned above, see [56,102]. When using ^{99m}Tc to label NPs or EVs it should be considered that this isotope may easily dissociate from the chelate it is bound to, such that the chelate is added in large excess in products used in the clinic in order to rebind the dissociated isotope [53]. One should also be aware of that dissociated ^{99m}Tc and other radioisotopes and chelates with these isotopes (e.g. obtained during degradation of the particles) often end up in the same organs as NPs [56].

Several authors have discussed that it is difficult and time-consuming to obtain sufficient amounts of EVs for drug delivery. This has led researchers to use so-called EV mimetics, produced from cells by e.g. sonication, electroporation, extrusion or freeze-thaw. These methods are also used to increase the loading capacity of drug or imaging agents, and to speed up the labelling procedure; reviewed in [11,24,107]. However, these treatments may result in major deformations of the membrane surface, including the generation of vesicles with an inverted membrane topology. Thus, it would not be surprising if these vesicles will have a biodistribution different from the EVs they should mimic. Moreover, the changes in the membrane structure expected in such EV mimetics will make it even more difficult to demonstrate reproducibility between batches, which is a challenge even for EVs with a normal topology [26].

Finally, we refer to an article by Pérez-Campaña *et al.* [108] who published that proton beam activation of metal oxide NPs could change ^{16}O to the PET isotope ^{13}N and thus make all metal oxide NPs detectable by PET. They claim that this method does not change the surface properties of the NPs, and that this is a simple and robust activation strategy that can be used for all metal oxide NPs.

4.2. Fluorescent labelling

As mentioned in the previous section, labels for biodistribution studies can either be covalently attached or just physically entrapped within the NPs or EVs. Fluorescent labelling of the particle surface may induce major changes of the surface properties and change the particle distribution. If the fluorescent substances are entrapped within the particles it should be considered that the detected fluorescent signals may be due to leakage of the fluorescent substance out of the particles [109]. Thus, it is important to select fluorophores that result in particle labelling being as stable as possible. Nile Red, which for many years was very popular for labeling of NPs, has been shown to be released from the lipophilic core of NPs, but by adding short alkyl chains to obtain NR668, a much better stability was obtained; discussion of this and the properties of many other fluorescent lipophilic dyes were recently reviewed [110]. It should be noted that it may be a challenge to quantify leakage of such fluorescent labels as these hydrophobic substances easily may adsorb to the glass or plastic equipment used during analyses. Also, if particles with such hydrophobic substances have entered cells, one should consider whether these dyes may be associated with the cells even after degradation of the particles. In addition to the challenges of quantifying the fluorescence signals of NPs and EVs as discussed above, one has to take into consideration that the intensity of the fluorescence may depend on the hydrophobicity/hydrophilicity in the surrounding of these labels, and also that the background fluorescence differs between various tissues [78]. Furthermore, it is important to use a low-fluorescence diet for studies based on fluorescence labeling.

We will finally in this section mention that the enzyme luciferase either bioengineered to be present inside EVs or chemically coupled to the surface of NPs or EVs can be used to obtain very strong light signals [111,112]. This method has, however, some major disadvantages. It is necessary to inject substrate molecules where the sensitive light signals are obtained as product of an enzymatic reaction. Thus, the time it takes for the substrate to reach the enzyme and the amount of substrate reaching the enzyme are important for the read-out. Also, repeated injection of at least some substrates might be toxic [102]. For a discussion about possibilities and challenges using bioluminescence imaging see [111]. One may also expect that chemical coupling of an enzyme to the surface of NPs or EVs may change their surface properties and thus the biodistribution of the particles.

4.3. Labelling for MRI or CT

The contrast agents used for MRI or CT are much less sensitive than the agents used for PET or SPECT as shown in Table 2. Some agents used for MRI or CT can theoretically be used for labelling of NPs or EVs in preclinical biodistribution studies. However, most of these agents give too weak signals to be really useful for labelling of such particles in clinical studies. Thus, development of new MRI active agents or more sensitive detector systems/protocols are needed to use MRI for biodistribution studies of NPs or EVs. As discussed in Section 3.2.2, the most commonly used contrast agents are low molecular weight Gd-chelates. Due to the possible association between the very small amounts of Gd retained in the body and the serious disorder nephrogenic systemic fibrosis [113], MR contrast research is focusing on improving the stability of such chelates more than in increasing their sensitivity [114]. Furthermore, making "Christmas trees" with many chelates bound together in the same molecule is likely to give large complexes that change the surface of the particle. It has been suggested to include iron oxide NPs in drug-containing NPs for theranostics. Such products will be more complicated to study and document for clinical use [27] and are not discussed in this article. However, it should

be mentioned that such NPs can be very useful for studies in small animals. Similarly, preclinical studies with theranostics may be performed using QDs for fluorescent imaging or heavy-metal based NPs for detection using X-rays. We do not see any other X-ray contrast agents being candidates for labelling of EVs or NPs. Thus, the use of MRI or CT in preclinical biodistribution studies are most useful when contributing with an anatomical image in combination with PET, SPECT or optical imaging. It should be noted that MRI provides a better differentiation and visualization of soft tissues than CT.

4.4. Comparison of labelling methods

Most articles in this field describe data obtained with one type of labelling in one type of particle, and it is therefore difficult to compare the data obtained in the various studies. However, Lázaro-Ibáñez *et al.* [112] compared data for biodistribution of EVs labelled with various methods and found several differences. Labelling was performed using the non-covalent hydrophobic fluorescent dye DiR, and by covalent modification of the surface by binding of ^{111}In-DTPA for SPECT-CT imaging. In addition, EVs were bioengineered to contain fluorescent (mCherry) or bioluminescent (luciferase) in their lumen by fusion to CD63. Whereas the mCherry labelling was found to give a too low signal-to-noise ratio to be useful, the luciferase labelling gave good signals when monitored *ex vivo*. However, the luciferase labelling changed the biodistribution and much higher signals were obtained from lungs compared to ^{111}In and DiR labelling, which as expected gave the strongest signals in liver and spleen. In our opinion, the data reported here for luciferase labeling is of special interest as similar data where reported from another group [115]. In both studies less than 5% of the signals obtained 4 h after injection were found in liver, and the signals estimated in lungs and spleen summed up to more than 90% of the total (reported as % per g tissue) with 2–4 times higher signal in lungs than spleen. These similarities were found even though different types of luciferase were conjugated to different proteins in different cell types and the injected EVs were detected using different substrates. The most likely interpretation of these results is that the luciferase method results in aggregation of the EVs in blood and then accumulation in the lungs, although this is difficult to understand since the enzyme was conjugated to proteins expected to be in the EV lumen. We wonder, however, if the cells respond by excreting the conjugated proteins via secretory autophagy, resulting in vesicles with an inverted membrane topology, similar to that recently published by Ariotti *et al.* [18].

Quantification performed by Lázaro-Ibáñez *et al.* [112] of signals obtained *ex vivo* for some key organs 4 and 24 h after injection of EVs labelled with ^{111}In or DiR are shown in Table 3 (containing organ weight data from [116]) and show some differences that may be of general interest regarding the use of these labelling methods. The ratios of liver/spleen signals are higher with the isotope labelling compared to the DiR labelling. As liver is by far the largest organ analyzed and the isotope is expected to penetrate tissue much better than light, it is likely that this difference is due to loss of light signals following penetration of thicker tissue. The amount of isotope found in the kidney was also very high compared to that found in spleen (and also compared with the DiR data). A possible explanation is that some ^{111}In or ^{111}In-DTPA has been detached from the EVs and then excreted through the kidneys. The authors reported that only small amounts of ^{111}In-DTPA were detected in urine and feces 24 h after injection and concluded that renal excretion did not contribute to the rapid clearance of radiolabeled EVs from the circulation (less than 10% remaining in blood 10 min after injection). Finally, DiR labelling resulted in higher recovery of the injected dose in lungs compared to that obtained with ^{111}In-DTPA labelling, indicating that there may be some aggregation of the DiR labelled EVs or some leakage of the dye in the first capillary system these EVs come in contact with. In summary, these data in our view nicely illustrate the challenge we still have to face regarding quantification of biodistribution data for EVs and NPs.

4.5. More critical discussions of published biodistribution data are needed

Based on the discussion in the previous sections it is obvious that we still need better methods for quantification of the biodistribution of *i.v.* injected NPs and EVs. Membrane permeable fluorophores (or some of the radioactive agents described in Section 4.1.) that label the lumen without being covalently bound to the liposomes or EVs, seem to be less stably associated with these particles than labels that are covalently coupled to the external surface of NPs or EVs. However, such surface modification is likely to change their biodistribution and should therefore be avoided. To improve these methods, it is essential that authors discuss their data more extensively. Too often, possible advantages of their method are discussed, but not challenges or possible pitfalls. Also, an evaluation/discussion of the uncertainty of the quantification of data is often missing. Furthermore, the NPs or EVs studied should be better characterized [25,27] as essential information for biodistribution studies such as comparison of size distribution, heterogeneity, impurities, charge and storage stability (including incubation in blood/plasma) before and after labelling are often missing. A more detailed characterization of the composition of EVs will also help to discriminate between different types of EVs, and the circulation time and biodistribution are likely to be different if PS (the "eat-me" signal) is present on the surface [26].

Although fluorescent-based imaging is by far the most used method for biodistribution studies in small animals and can give important information about the biodistribution of NPs and EVs,

Table 3
Biodistribution of EVs labelled with different methods. Quantification performed *ex vivo* 4 and 24 h after *i.v.* injection in tumor-bearing BALB/c mice. Data from Lázaro-Ibáñez *et al.* [112].

Organ	^{111}In [1]		DiR[2]		Organ weight (g)[3]
	4 h	24 h	4 h	24 h	
Liver	45	78	100	~85	1.75
Spleen	33	25	~93	100	0.1
Kidney	7	12	~7	~3	0.32
Lungs	2–3	~1	~40	~13	0.12

[1]Added as ^{111}In-DTPA covalently bound to the surface. Data given were obtained using gamma counting and reported as percent of the injected dose per g tissue (%ID/g). The values reported show these mice to be small with a liver weight of ~0.9 g. Data for lungs are estimated by us from their Fig. 3.
[2]DiR was noncovalently added bound to the EVs. The data shown in their Fig. 2G (obtained using an IVIS Lumina system) as total radiant efficiency per g tissue have been recalculated such that the highest signal obtained (spleen) is set to 100%.
[3]Organ weight data are from Davies and Morris [116]; these data for 20 g mice are shown to illustrate the size differences of these organs.

it is in practice not possible to obtain quantitative data based on this labelling. The only way to obtain quantitative whole-body biodistribution data is to label with radioisotopes for PET or SPECT imaging, which means that highly specialized equipment and competence are needed.

When interpreting biodistribution data it is important to be aware of that detection in urine of substances used to label NPs or EVs larger than 10–20 nm is most likely due to that the label is no longer associated with the injected particles. Then it is also necessary to consider if labels detected in the kidneys could be free or part of degradation products, i.e. not demonstrating the presence of intact particles. It should be noted that the low-molecular weight contrast agents used for CT or MRI in the clinic are almost completely excreted via kidneys within 24 h after injection in humans and even faster in small animals. The observation of significant differences in the rapid excretion in urine of the free label and labelled particles clearly demonstrates that particles have been labelled. However, several samples taken different times after injection should be analyzed before concluding that the data support successful radiolabeling. If high levels of the labels are detected in lungs, it should be considered that the particles may have aggregated following injection in blood or that the labels could have dissociated from the particles and are taken up in the first capillary network these particles enter. We have observed major differences in the biodistribution of NPs made of very similar monomers and having similar physiochemical characteristics [117], demonstrating that it is difficult to foresee the biodistribution of new NPs. Further details about uptake of NPs or EVs into liver and spleen is discussed in Section 6.

5. Chemical analyses of biological samples

In this section we discuss different methods to analyze biological samples such as homogenates of isolated tissues, blood, urine and feces that can throw light on the biodistribution and excretion of NPs and EVs. This includes studies of constituents, drugs or imaging agents that can be used in part to describe the biodistribution of these particles or substances that were associated with them at the time of injection. It is important to discuss whether the signals observed are expected to be due to the presence of the injected NPs or EVs or if the signals detected are due to molecules/atoms no longer associated with these particles.

5.1. Radioactivity measurements

Radioactivity measurements can be performed with practically all types of biological material, including blood, urine, feces and tissue samples using radioactive isotopes and a scintillation counter or gamma counter for detection and quantification of these isotopes. Quenching in the sample may be a problem with such quantification, making it important to use quenching curves when performing the quantifications. So-called sample oxidizers can be useful for quantification of substances labelled with ^{3}H and/or ^{14}C, as the samples will be totally combusted, and the two isotopes will be physically separated. Thus, all ^{3}H ends up in one fraction as $^{3}H_2O$ and all ^{14}C ends up in another fraction as $^{14}CO_2$ such that these isotopes can be quantified in the same sample without any quenching.

5.2. Fluorescence

Quantification of the amount of fluorescence in a solution can be performed by many different types of equipment available in most laboratories. Quantitative analyses of fluorescence are in principle both sensitive and rapid to perform [118]. We discussed above several challenges regarding quantification of fluorescence signals when performing imaging of whole body or organs/tissues. Similar challenges should also be considered if the goal is to obtain quantitative data from other type of studies, and we refer to an excellent review regarding pitfalls and opportunities in quantitative fluorescence-based studies [119].

5.3. Mass spectrometry (MS)

MS is based on measuring the mass-to-charge ratio of ions in a sample that is ionized, e.g. by bombarding it with a beam of electrons. This is a valuable technique to identify and quantify specific molecules or fragments of these molecules. It is often used in combination with a chromatographic step to separate various types of substances to be analyzed, e.g. in combination with liquid chromatography (LC-MS). Since this technique both has a very high sensitivity and can identify most molecules present in biological samples it is a commonly applied technique during drug development studies, including ADME and PK studies. MS or LC-MS analyses are often used to demonstrate that drugs entrapped in NPs are circulating longer in blood than the free drug and to estimate the blood kinetics of drugs. Discussion of the data obtained in such studies should include if the method is able to discriminate between drug still entrapped within the NPs and drug released from the NPs, i.e. being free and able to exert its biological activity. In the draft guidance mentioned above [2], it is stated that "In general, total, free, and nanomaterial-associated drug should be measured separately or indirectly derived. This may require separation of free and nanomaterial-associated drug prior to detection or simultaneous analysis". In fact, it is often a challenge also to study the release of drugs from NPs during storage of the product, as the released, often very hydrophobic, drug may stick to the containers used for storage or analyses.

To our knowledge there is only one article describing a method to measure the release of drugs from NPs in biological matrices. The method involves spiking with a stable isotope-labeled drug into the plasma samples containing the NPs. The labelled drug equilibrates with the normo-isotopic drug released from the nanomedicine, and analysis of the ultrafiltrate fraction of the isotope-labelled and unlabeled drug can be used to measure how much of the normo-isotopic drug that is free in plasma. Then it is possible to calculate how much of the drug is encapsulated or free [120]. This is an elegant method that should be very useful for development and regulatory evaluation of such products, including comparing properties of the so-called generic bioequivalent products. However, this method is very complicated and time consuming and it cannot be expected to be included in early basic studies.

5.4. Inductively coupled plasma mass spectrometry (ICP-MS)

ICP-MS analyses can be used to obtain high sensitivity and measure a wide dynamic range of most elements in the periodic table; it is also possible to analyze many elements at the same time following an easy sample preparation [121,122]. Thus, this method can be applied for analyses of e.g. Au, Fe and many other metals. Among the few elements found in biological samples and not suited for ICP-MS analyses are H, C, N, O, F and Cl [121]. Since ICP-MS detects the mass of each element, one can quantify various isotopes of one element. One isotope that may be of interest for analyses of particles in biological matrixes is ^{58}Fe; this non-radioactive isotope constitutes only 0.28% of total Fe isotopes. Since it can be enriched and added in e.g. iron oxide-based NPs it can in principle be used as a very sensitive method to measure injected Fe in the presence of high amounts of endogenous Fe.

As mentioned above, SPECT imaging is most often performed using ^{99m}Tc with a half-life of 6 h. This isotope can also be quanti-

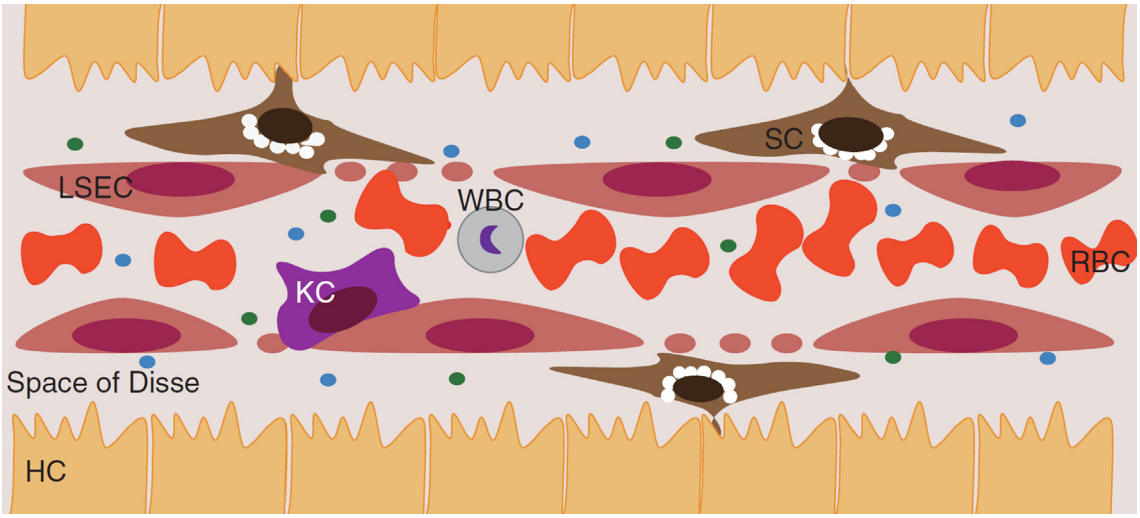

Fig. 9. Cartoon of the liver sinusoid illustrating the localization of the main cell types. Hepatocytes (HC), liver sinusoidal endothelial cells (LSECs), the liver resident macrophages or Kupffer cells (KC) and the stellate cells (SC): SC are located in the space of Disse. Also shown in the cartoon are red blood cells (RBC) and white blood cells (WBC). The small dots can be macromolecules, NPs or EVs. This cartoon is a copy of Fig. 2 in [32] reproduced with approval from John Wiley and Sons. (For interpretation of the references to colour in this figure legend, the reader is referred to the web version of this article.)

fied in biological samples using gamma counting with correction of disintegration at the time of analysis. Another possibility to measure the amounts of such agents present in e.g. blood and urine samples is to benefit from the very high sensitivity of ICP-MS for analysis of the non-radioactive ^{99}Tc [121]. We are not aware of any studies benefiting from ICP-MS analysis of substances labelled with non-radioactive Tc. However, one of us was several years ago involved in a study (not published) demonstrating a limit of quantification of 10–20 pg/ml of Tc in blood and urine following injection in rats. Thus, this approach should make it possible to perform part of biodistribution studies with non-radioactive Tc-labeled substances, and also to measure Tc-content of samples so long time after injection of ^{99m}Tc-labelled substance that it is not possible to quantify by gamma counting.

5.5. Magnetic resonance spectroscopy (MRS)

MRS can be used to identify and quantify many substances in biological tissue/samples. This technique can be used to study PK of drugs labelled with MR detectable nuclei such as ^{13}C or ^{19}F. High-resolution magic angle spinning MRS is a relatively new technology that can be used for analyzing the metabolome of tissue biopsies. For further information regarding the use of MRS to study biological samples, see [123].

6. Similarities and differences expected in the biodistribution of NPs and EVs

Phagocytes are expected to play a major role in the clearance of particles, including i.v. injected NPs and EVs, and several studies during recent years have shown a similar biodistribution of *i.v.* injected EVs as that reported earlier for NPs. Thus, a major amount of the injected dose of EVs accumulates in liver, but the uptake in spleen is also important [124,125] and is often higher than in liver when quantifying the uptake per g tissue. In addition, uptake by lungs are often reported to be high, but as discussed above this could in some cases be due to aggregation of particles or leakage of fluorescence from the particles.

Both liver and spleen can take up particles with a large variation in size. Although one should be careful when concluding which organs and cells are most efficient in taking up particles of a given size, it looks like liver is more effective than spleen in taking up NPs up to 200 nm, whereas spleen is more effective in taking up even larger NPs [125]. So far most studies describing uptake of NPs into liver have focused on the uptake by Kupffer cells, although there are several studies indicating that the LSEC may be similar or perhaps more important than Kupffer cells for liver uptake of NPs smaller than 100 nm [14,32,124]. Also, particles smaller than the size of liver fenestrae may extravasate into the space of Disse (Fig. 9) where they can interact with the hepatocytes. Estimates of how the various liver cells contribute to the total cell number and liver volume are given in Table 4 (some of these data are reproduced from [126]). For more information about the function and endocytic activity of liver cells, see [32,127]. In summary, more studies are required to understand the contribution of Kupffer cells, LSEC and hepatocytes to the total liver uptake of NPs and EVs with various sizes and surface properties and to learn more about the contribution of liver versus spleen for such uptake.

As mentioned above, PS present on the surface of cells/vesicles has for a long time been known as an "eat me" signal for phagocytes. Also, for several years now, CD47, which is present in all human cells, has been known to be a "don't eat me" signal by starting reactions that depress the phagocytic activity [128]. CD47 has also been reported to be present on the surface of at least some EVs, and an enhanced retention of exosomes compared to liposomes in circulation following intraperitoneally injection was suggested to be due to the presence of CD47 on exosomes [129]. We are not aware of any studies describing if PS or CD47 provides the most dominant effect, or if the effect of CD47 will differ depending on whether the EVs have PS on the surface or not. It should be noted that several other "eat me" or "don't eat me" signals have been reported regarding clearance of dying cells [130], but we are not aware of any discussions regarding the effect of

Table 4
Cellular composition of rat liver cells reported as percent of total liver cell number and liver cell volume. Data from [126] and https://dliver.com/size-matters.

Liver cells	% of total liver cell number	% of liver cell volume
Hepatocytes	60–70	>90
LSECs	21	3.3
Kupffer cells	8.5	2.5
Stellate cells	5.5	1.6

these other signals for the biodistribution of NPs or EVs. We are not aware of any reports where researchers have tried to study if addition of PEG chains can hide or influence the effect of such "eat me" or "don't eat me" signals on clearance from circulation.

Discussions about whether the protein corona, i.e. binding of proteins to NPs, can affect the *in vivo* behavior of the NPs have been ongoing for many years. The protein corona described in these studies often contains proteins involved in complement activation, blood coagulation, macrophage uptake, and lipid metabolism [117]. The discussions include how these proteins can contribute to differences in PK, biodistribution, cellular uptake, and biological effects of the NPs. Notably, it has been reported that there are differences between the protein corona obtained *in vitro* (mice plasma) and *in vivo* in mice [131]. Thus, more studies are needed to investigate if or to which extent characterization of the protein corona can explain the *in vivo* behavior of NPs.

Finally, we would like to mention that there are several reports describing that the amount of drug-containing NPs homing to e.g. tumors can be increased by "saturating" the liver uptake by pre-injection of other NPs [132–134]. A similar idea was recently reported for EVs; an elevated number of circulating EVs were found in mice receiving a high fat diet, and these mice showed a decreased uptake of EVs by Kupffer cells and LSEC [135].

7. Animal species and models used in preclinical studies

7.1. Animal species

To document efficacy and safety for regulatory approval of new drugs to be injected in humans, the drug has to be studied in two other species, normally one rodent and one non-rodent, before testing in humans. Most often rats and beagle dogs are used, although in some cases also primates are used. Pigs are also often used as they show several similar anatomic and physiological characteristics to humans regarding e.g. the cardiovascular, urinary and digestive systems [136]. Pigs have, however, one major drawback as animal model for *i.v.* injection of particles, because they have intravascular macrophages in the lungs, typical for cloven-hoofed animals. We have previously discussed problems revealed in a late development phase due to injection of particles in pigs. Following injection of an ultrasound contrast agent (Albunex, albumin-based air-filled microspheres) the pig obtained massive increase in the pulmonary pressure and a decline in the systemic arterial pressure, and died after repeated injections [137]. However, at that stage this agent had already been injected in several hundred people in clinical trials without observing any cardiovascular effects. Injection of the ^{125}I-labelled agent in pigs resulted in 90% of the injected dose ending up in lungs, whereas in rats 60% of the injected dose ended up in liver and only 5% in lungs. As discussed in [137] it was concluded that the effect in pigs was due to release of thromboxane A2 from the intravascular pulmonary macrophages. For further discussions regarding uptake of different particles by the intravascular pulmonary macrophages in various species, see [138,139].

When choosing which species to use for preclinical testing in basic research laboratories it is important that less substance is needed for testing in the smallest animals. Often one also wants to compare several substances and only small amounts of some of the substances may be available. When planning such experiments the physiological parameters given for mice, rats, rabbits, rhesus monkey, dog and humans (including organ weights and blood volume) by Davies and Morris [116] are very valuable.

7.2. Animal models

It may be a challenge to select which animal model to use when studying the therapeutic effect of drugs in preclinical studies, reviewed in [140]. Some aspects of selection of species to be used for ADME studies was discussed in the previous section. Most *in vivo* studies performed with NPs or EVs for cancer therapy are done using immunodeficient mice with solid tumors. Formation of tumors following subcutaneous injection of cells from various cancer cell lines are most common. Such cells often show a rapid tumor growth and these tumors normally show a tissue structure very different from their human counterparts, including severely altered microenvironment and changes in the vascular, lymphatic and immune compartments. Patient-derived xenografts (PDXs) are generated by subcutaneous implantation of surgically derived materials from human tumors into immunodeficient mice and may better simulate the human tumor microenvironment than tumors formed following injection of cells. It should be noted that the use of immunocompromised mice, which is required for successful engraftment of the PDX, precludes the possibility to study immune cell function. An orthotopically transplanted PDX means that the tumor is placed in the natural anatomical site. We refer to the following review articles for further information regarding various tumor models in mice [141,142].

Tumor models in animals are of course needed if the goal is to study the therapeutic effect of drug-containing particles. Such models are also useful to estimate and compare the amount of different injected particles that end up in the tumor. We find it, however, important to stress that since very little of the injected dose (in most cases not more than 1%) ends up in tumors, one can expect the biodistribution data to be very similar after injection of NPs or EVs in mice with or without tumor.

7.3. Usefulness of NPs or EVs for imaging or therapy

Most of the discussion in this article has been related to opportunities and challenges when studying the biodistribution of NPs and EVs. A future goal for studies of drug-containing NPs will be to follow both the NPs or its constituents as well as the drug. For the therapeutic effect, it is not the particles themselves that are important, but the active pharmaceutical ingredient they carry and that the active substances get access to their targets. The drug could have left the particles before the time-point for the biodistribution measurement, or it may still be entrapped within the particles in a form where it is not able to reach its target. Thus, more NPs or EVs reaching a target does not mean that more drug is available at the target; see discussion by Scott McNeil [38]. Also, even if only very little of the injected dose is reaching the target, it may still be enough to give a good therapeutic effect. For example, although less than 1% of the injected dose of Doxil®/Caelyx® (the first NP-based product that reached the market; liposomes containing doxorubicin) was detected in tumors, that was still much more than detected in tumors following injection of free doxorubicin [143].

The data published so far show that most NPs end up in liver and often with similar amounts of NPs per g tissue in spleen. Imaging data also show that several NPs end up in high concentrations in lymph nodes. As discussed above there are often also high signals from NPs detected in lungs and kidneys, although the origin of these signals should be carefully evaluated. These tissues, tumors and regions of inflammation are thus among the most interesting areas to benefit from the use of NPs or EVs for drug delivery. Regarding the possible use of such particles for imaging we believe that it is most likely that they can be favorably used for imaging of liver, spleen and lymph nodes. As discussed by us earlier [27,48], authors of many of the studies describing the use of NPs for medical imaging lack knowledge about what is needed to bring such products into clinical use and should therefore benefit from collaborating with scientists having that knowledge.

Regarding the possible use of NPs for medical imaging, we refer to an excellent review by Kiessling *et al.* [144].

When considering the use of NPs or EVs for drug delivery, it is important to take into consideration the long list of studies needed for obtaining approval for such use and also the risk/benefit analyses one can expect pharmaceutical companies to perform before starting development of new products [27]. Included in such evaluations is that less adverse effects are accepted for an imaging agent to be used in healthy individuals compared to agents delivering a life-saving drug to patients. Thus, it is more likely that such particles will be useful to deliver therapeutics than to deliver imaging agents. Many scientists focus on the possibility to make theranostics, i.e. to use the same product both for therapy and imaging. This is a very useful approach for preclinical studies. However, the ideal properties for products to deliver therapeutics and imaging agents are different (discussed above), and it will be more complicated to produce reproducible batches of theranostics than to produce products focusing on just one of the possible uses. Thus, we are not convinced that theranostics will end up being as useful in the clinic as in preclinical studies [27].

8. Conclusions and future perspectives

We have in the present article discussed opportunities, challenges and pitfalls when studying the biodistribution, degradation and excretion of NPs and EVs. Although major improvements have been obtained during recent years, we have still much to learn about such processes and the interaction between NPs/EVs and cells/tissues. The best way forward is in our opinion that authors publish more detailed data about the characterization and stability of the particles studied, and also discuss not only the advantages, but also the challenges and draw-backs of the methods and materials used. Today only ICP-MS measurements of stable inorganic NPs can be used to obtain quantitative measurements of the amounts of NPs in selected organs/tissues.

Presently, fluorescent labeling is the most common method to study the biodistribution of NPs or EVs in mice, but as discussed in this article there are several challenges/pitfalls with that approach. Labelling with radioisotopes and imaging using PET or SPECT have several advantages regarding quantification, but also with such analyses it is not possible to make sure whether the label is still connected to the injected substance at the time of analysis and whether the labelling method has changed the surface properties and thus the biodistribution of the injected particles. In the scientific literature one can often see the statement "Seeing is believing". Regarding the issues discussed in this review it might be beneficial to add the following question: What do we actually see, the particles or just released labels?

Finally, if the intention is to bring such NPs or EVs into clinical use it is important to have an interdisciplinary collaboration between scientists from chemistry, biology, pharmacology, toxicology, medicine and people with experience from pharmaceutical industry.

Declaration of Competing Interest

The authors declare that they have no known competing financial interests or personal relationships that could have appeared to influence the work reported in this paper.

Acknowledgements

The authors have been supported by the Norwegian Cancer Society, the Research Council of Norway and the South Eastern Norway Regional Health Authority.

References

[1] M.A. Hamburg, Science and regulation. FDA's approach to regulation of products of nanotechnology, Science 336 (2012) 299–300.
[2] Guidance for industry (Draft guidance): Drug products, including biological products, that contain nanomaterials, (2017).
[3] Guidance for Industry. Developing medical imaging drug and biological products. Part 1: Conducting safety assessments, 2004.
[4] FDA, Public safety notification on exosome products, 2019. https://www.fda.gov/vaccines-blood-biologics/safety-availability-biologics/public-safety-notification-exosome-products.
[5] M.J. Mitchell, M.M. Billingsley, R.M. Haley, M.E. Wechsler, N.A. Peppas, R. Langer, Engineering precision nanoparticles for drug delivery, Nat. Rev. Drug Discov. 20 (2021) 101–124.
[6] M. Haider, S.M. Abdin, L. Kamal, G. Orive, Nanostructured Lipid Carriers for Delivery of Chemotherapeutics: A Review, Pharmaceutics 12 (2020).
[7] Y.H. Chung, V. Beiss, S.N. Fiering, N.F. Steinmetz, COVID-19 Vaccine Frontrunners and Their Nanotechnology Design, ACS Nano 14 (2020) 12522–12537.
[8] Y. Barenholz, Doxil(R)–the first FDA-approved nano-drug: lessons learned, J. Control. Release 160 (2012) 117–134.
[9] Y. Liu, Z. Mei, L. Mei, J. Tang, W. Yuan, S. Srinivasan, R. Ackermann, A.S. Schwendeman, Analytical method development and comparability study for Am Bisome(R) and generic Amphotericin B liposomal products, Eur. J. Pharm. Biopharm. 157 (2020) 241–249.
[10] L. van der Koog, T.B. Gandek, A. Nagelkerke, Liposomes and Extracellular Vesicles as Drug Delivery Systems: A Comparison of Composition, Pharmacokinetics, and Functionalization, Adv. Healthc. Mater. (2021) e2100639.
[11] S. Le Saux, A. Aubert-Pouessel, K.E. Mohamed, P. Martineau, L. Guglielmi, J.M. Devoisselle, P. Legrand, J. Chopineau, M. Morille, Interest of extracellular vesicles in regards to lipid nanoparticle based systems for intracellular protein delivery, Adv. Drug Deliv. Rev. 176 (2021) 113837.
[12] B.L. Banik, P. Fattahi, J.L. Brown, Polymeric nanoparticles: the future of nanomedicine, Wiley Interdiscip. Rev. Nanomed. Nanobiotechnol. 8 (2016) 271–299.
[13] T. Skotland, P.C. Sontum, I. Oulie, In vitro stability analyses as a model for metabolism of ferromagnetic particles (Clariscan), a contrast agent for magnetic resonance imaging, J. Pharm. Biomed. Anal. 28 (2002) 323–329.
[14] K. Briley-Saebo, A. Bjornerud, D. Grant, H. Ahlstrom, T. Berg, G.M. Kindberg, Hepatic cellular distribution and degradation of iron oxide nanoparticles following single intravenous injection in rats: implications for magnetic resonance imaging, Cell Tissue Res. 316 (2004) 315–323.
[15] C. Corot, P. Robert, J.M. Idee, M. Port, Recent advances in iron oxide nanocrystal technology for medical imaging, Adv. Drug Deliv. Rev. 58 (2006) 1471–1504.
[16] K.T. Yong, W.C. Law, R. Hu, L. Ye, L. Liu, M.T. Swihart, P.N. Prasad, Nanotoxicity assessment of quantum dots: from cellular to primate studies, Chem. Soc. Rev. 42 (2013) 1236–1250.
[17] T. Skotland, N.P. Hessvik, K. Sandvig, A. Llorente, Exosomal lipid composition and the role of ether lipids and phosphoinositides in exosome biology, J. Lipid Res. 60 (2019) 9–18.
[18] N. Ariotti, Y. Wu, S. Okano, Y. Gambin, J. Follett, J. Rae, C. Ferguson, R.D. Teasdale, K. Alexandrov, F.A. Meunier, M.M. Hill, R.G. Parton, An inverted CAV1 (caveolin 1) topology defines novel autophagy-dependent exosome secretion from prostate cancer cells, Autophagy 17 (2021) 2200–2216.
[19] I. Shlomovitz, M. Speir, M. Gerlic, Flipping the dogma - phosphatidylserine in non-apoptotic cell death, Cell Commun Signal 17 (2019) 139.
[20] Y.N. Gong, J.C. Crawford, B.L. Heckmann, D.R. Green, To the edge of cell death and back, FEBS J. 286 (2019) 430–440.
[21] F.J. Verweij, L. Balaj, C.M. Boulanger, D.R.F. Carter, E.B. Compeer, G. D'Angelo, S. El Andaloussi, J.G. Goetz, J.C. Gross, V. Hyenne, E.M. Kramer-Albers, C.P. Lai, X. Loyer, A. Marki, S. Momma, E.N.M. Nolte-'t Hoen, D.M. Pegtel, H. Peinado, G. Raposo, K. Rilla, H. Tahara, C. Thery, M.E. van Royen, R.E. Vandenbroucke, A. M. Wehman, K. Witwer, Z. Wu, R. Wubbolts, G. van Niel, The power of imaging to understand extracellular vesicle biology in vivo, Nat. Methods 18 (2021) 1013–1026.
[22] O.P.B. Wiklander, M. Brennan, J. Lötvall, X.O. Breakefield, S. El Andaloussi, Advances in therapeutic applications of extracellular vesicles, Sci. Transl. Med. 11 (2019) eaav 8521.
[23] R. Kalluri, V.S. LeBleu, The biology, function, and biomedical applications of exosomes, Science, 367 (2020) eaau 6977.
[24] W. Meng, C. He, Y. Hao, L. Wang, L. Li, G. Zhu, Prospects and challenges of extracellular vesicle-based drug delivery system: considering cell source, Drug Deliv 27 (2020) 585–598.
[25] P. Escude Martinez de Castilla, L. Tong, C. Huang, A.M. Sofias, G. Pastorin, X. Chen, G. Storm, R.M. Schiffelers, J.W. Wang, Extracellular vesicles as a drug delivery system: A systematic review of preclinical studies, Adv Drug Deliv Rev, 175 (2021) 113801.
[26] T. Skotland, K. Sagini, K. Sandvig, A. Llorente, An emerging focus on lipids in extracellular vesicles, Adv. Drug Deliv. Rev. 159 (2020) 308–321.
[27] T. Skotland, T.G. Iversen, K. Sandvig, Development of nanoparticles for clinical use, Nanomedicine (Lond) 9 (2014) 1295–1299.
[28] F. Royo, U. Cossio, A. Ruiz de Angulo, J. Llop, J.M. Falcon-Perez, Modification of the glycosylation of extracellular vesicles alters their biodistribution in mice, Nanoscale 11 (2019) 1531–1537.

[29] F. Braet, E. Wisse, Structural and functional aspects of liver sinusoidal endothelial cell fenestrae: a review, Comp Hepatol 1 (2002) 1.
[30] M. Gaumet, A. Vargas, R. Gurny, F. Delie, Nanoparticles for drug delivery: the need for precision in reporting particle size parameters, Eur. J. Pharm. Biopharm. 69 (2008) 1–9.
[31] D.G. Le Couteur, A. Warren, V.C. Cogger, B. Smedsrod, K.K. Sorensen, R. De Cabo, R. Fraser, R.S. McCuskey, Old age and the hepatic sinusoid, Anat Rec (Hoboken) 291 (2008) 672–683.
[32] K.K. Sorensen, J. Simon-Santamaria, R.S. McCuskey, B. Smedsrod, Liver Sinusoidal Endothelial Cells, Compr Physiol 5 (2015) 1751–1774.
[33] Y. Matsumura, H. Maeda, A new concept for macromolecular therapeutics in cancer chemotherapy: mechanism of tumoritropic accumulation of proteins and the antitumor agent smancs, Cancer Res. 46 (1986) 6387–6392.
[34] L.E. Gerlowski, R.K. Jain, Microvascular permeability of normal and neoplastic tissues, Microvasc. Res. 31 (1986) 288–305.
[35] S. Sindhwani, A.M. Syed, J. Ngai, B.R. Kingston, L. Maiorino, J. Rothschild, P. MacMillan, Y. Zhang, N.U. Rajesh, T. Hoang, J.L.Y. Wu, S. Wilhelm, A. Zilman, S. Gadde, A. Sulaiman, B. Ouyang, Z. Lin, L. Wang, M. Egeblad, W.C.W. Chan, The entry of nanoparticles into solid tumours, Nat. Mater. 19 (2020) 566–575.
[36] T. Skotland, K. Sandvig, Transport of nanoparticles across the endothelial cell layer, Nano Today 36 (2021) 101029.
[37] S. Wilhelm, A.J. Tavares, Q. Dai, S. Ohta, J. Audet, H.F. Dvorak, W.C. Chan, Analysis of nanoparticle delivery to tumours, Nat. Rev. Mater. 1 (2016) 16014.
[38] S.E. McNeil, Evaluation of nanomedicine: stick to basics, Nat. Rev. Mater. 1 (2016) 16073.
[39] T. Lammers, F. Kiessling, M. Ashford, W. Hennink, D. Crommelin, G. Storm, Cancer nanomedicine: Is targeting our target?, Nat Rev. Mater. 1 (2016) 16069.
[40] D.M. Goldenberg, Advancing role of radiolabeled antibodies in the therapy of cancer, Cancer Immunol. Immunother. 52 (2003) 281–296.
[41] M.R. Pollak, S.E. Quaggin, M.P. Hoenig, L.D. Dworkin, The glomerulus: the sphere of influence, Clin. J. Am. Soc. Nephrol. 9 (2014) 1461–1469.
[42] H.S. Choi, W. Liu, P. Misra, E. Tanaka, J.P. Zimmer, I.B. Itty, M.G. Bawendi, J.V. Frangioni, Renal clearance of quantum dots, Nat. Biotechnol. 25 (2007) 1165–1170.
[43] M.L. Torgersen, P.J. Judge, J.F. Bada Juarez, A.D. Pandya, M. Fusser, C.W. Davies, M.K. Maciejewska, D.J. Yin, G.M. Maelandsmo, T. Skotland, A. Watts, K. Sandvig, Physicochemical Characterization, Toxicity and In Vivo Biodistribution Studies of a Discoidal, Lipid-Based Drug Delivery Vehicle: Lipodisq Nanoparticles Containing Doxorubicin, J. Biomed. Nanotechnol. 16 (2020) 419–431.
[44] C.F. Adhipandito, S.H. Cheung, Y.H. Lin, S.H. Wu, Atypical Renal Clearance of Nanoparticles Larger Than the Kidney Filtration Threshold, Int. J. Mol. Sci. 22 (2021) 11182.
[45] G. Sonavane, K. Tomoda, K. Makino, Biodistribution of colloidal gold nanoparticles after intravenous administration: effect of particle size, Colloids Surf. B Biointerfaces 66 (2008) 274–280.
[46] W.H. De Jong, W.I. Hagens, P. Krystek, M.C. Burger, A.J. Sips, R.E. Geertsma, Particle size-dependent organ distribution of gold nanoparticles after intravenous administration, Biomaterials 29 (2008) 1912–1919.
[47] R.M. Steinman, I.S. Mellman, W.A. Muller, Z.A. Cohn, Endocytosis and the recycling of plasma membrane, J. Cell Biol. 96 (1983) 1–27.
[48] T. Skotland, T.G. Iversen, K. Sandvig, New metal-based nanoparticles for intravenous use: requirements for clinical success with focus on medical imaging, Nanomedicine 6 (2010) 730–737.
[49] M.J. Ernsting, M. Murakami, A. Roy, S.D. Li, Factors controlling the pharmacokinetics, biodistribution and intratumoral penetration of nanoparticles, J. Control. Release 172 (2013) 782–794.
[50] N. Hoshyar, S. Gray, H. Han, G. Bao, The effect of nanoparticle size on in vivo pharmacokinetics and cellular interaction, Nanomedicine (Lond) 11 (2016) 673–692.
[51] T.G. Iversen, T. Skotland, K. Sandvig, Endocytosis and intracellular transport of nanoparticles: Present knowledge and need for future studies, Nano Today 6 (2011) 176–185.
[52] B.B. Goldberg, D.A. Merton, J.B. Liu, G. Murphy, F. Forsberg, Contrast-enhanced sonographic imaging of lymphatic channels and sentinel lymph nodes, J. Ultrasound Med. 24 (2005) 953–965.
[53] T. Skotland, Molecular imaging: challenges of bringing imaging of intracellular targets into common clinical use, Contrast. Media, Mol. Imaging 7 (2012) 1–6.
[54] A.K. Shukla, U. Kumar, Positron emission tomography: An overview, J Med Phys 31 (2006) 13–21.
[55] M. Unterrainer, C. Eze, H. Ilhan, S. Marschner, O. Roengvoraphoj, N.S. Schmidt-Hegemann, F. Walter, W.G. Kunz, P.M.A. Rosenschold, R. Jeraj, N.L. Albert, A.L. Grosu, M. Niyazi, P. Bartenstein, C. Belka, Recent advances of PET imaging in clinical radiation oncology, Radiat Oncol 15 (2020) 88.
[56] J. Pellico, P.J. Gawne, T.M.d.R. R, Radiolabelling of nanomaterials for medical imaging and therapy, Chem Soc Rev, 50 (2021) 3355-3423.
[57] Y. Ming, N. Wu, T. Qian, X. Li, D.Q. Wan, C. Li, Y. Li, Z. Wu, X. Wang, J. Liu, N. Wu, Progress and Future Trends in PET/CT and PET/MRI Molecular Imaging Approaches for Breast Cancer, Front. Oncol. 10 (2020) 1301.
[58] M.R. Mirbolooki, C.C. Constantinescu, M.L. Pan, J. Mukherjee, Quantitative assessment of brown adipose tissue metabolic activity and volume using 18F-FDG PET/CT and & #946;3-adrenergic receptor activation, EJNMMI Res 1 (2011) 30.
[59] M.M. Khalil, J.L. Tremoleda, T.B. Bayomy, W. Gsell, Molecular SPECT Imaging: An Overview, Int J Mol Imaging 2011 (2011) 796025.
[60] O. Israel, O. Pellet, L. Biassoni, D. De Palma, E. Estrada-Lobato, G. Gnanasegaran, T. Kuwert, C. la Fougere, G. Mariani, S. Massalha, D. Paez, F. Giammarile, Two decades of SPECT/CT - the coming of age of a technology: An updated review of literature evidence, Eur. J. Nucl. Med. Mol. Imaging 46 (2019) 1990–2012.
[61] Technetium-99m generator. https://en.wikipedia.org/wiki/Technetium-99m_generator. Access data: April 22, 2022.
[62] M. Uenomachi, M. Takahashi, K. Shimazoe, H. Takahashi, K. Kamada, T. Orita, K. Ogane, A.B. Tsuji, Simultaneous in vivo imaging with PET and SPECT tracers using a Compton-PET hybrid camera, Sci. Rep. 11 (2021) 17933.
[63] Y. Jeong, H.S. Hwang, K. Na, Theranostics and contrast agents for magnetic resonance imaging, Biomater. Res. 22 (2018) 20.
[64] A.P. Khandhar, R.M. Ferguson, H. Arami, K.M. Krishnan, Monodisperse magnetite nanoparticle tracers for in vivo magnetic particle imaging, Biomaterials 34 (2013) 3837–3845.
[65] J.E. Rosen, L. Chan, D.B. Shieh, F.X. Gu, Iron oxide nanoparticles for targeted cancer imaging and diagnostics, Nanomedicine 8 (2012) 275–290.
[66] S.M. Dadfar, K. Roemhild, N.I. Drude, S. von Stillfried, R. Knuchel, F. Kiessling, T. Lammers, Iron oxide nanoparticles: Diagnostic, therapeutic and theranostic applications, Adv. Drug Deliv. Rev. 138 (2019) 302–325.
[67] S. Zanganeh, G. Hutter, R. Spitler, O. Lenkov, M. Mahmoudi, A. Shaw, J.S. Pajarinen, H. Nejadnik, S. Goodman, M. Moseley, L.M. Coussens, H.E. Daldrup-Link, Iron oxide nanoparticles inhibit tumour growth by inducing pro-inflammatory macrophage polarization in tumour tissues, Nat. Nanotechnol. 11 (2016) 986–994.
[68] H. Arami, A. Khandhar, D. Liggitt, K.M. Krishnan, In vivo delivery, pharmacokinetics, biodistribution and toxicity of iron oxide nanoparticles, Chem. Soc. Rev. 44 (2015) 8576–8607.
[69] H. Lusic, M.W. Grinstaff, X-ray-computed tomography contrast agents, Chem. Rev. 113 (2013) 1641–1666.
[70] X. Li, N. Anton, G. Zuber, T. Vandamme, Contrast agents for preclinical targeted X-ray imaging, Adv. Drug Deliv. Rev. 76 (2014) 116–133.
[71] Medical ultrasound. https://en.wikipedia.org/wiki/Medical_ultrasound. Access data: April 22, 2022.
[72] A. Ignee, N.S. Atkinson, G. Schuessler, C.F. Dietrich, Ultrasound contrast agents, Endosc, Ultrasound 5 (2016) 355–362.
[73] C.M. Moran, A.J.W. Thomson, Preclinical Ultrasound Imaging—A Review of Techniques and Imaging Applications, Front. Phys. 8 (2020) 124.
[74] B. Theek, M. Baues, T. Ojha, D. Mockel, S.K. Veettil, J. Steitz, L. van Bloois, G. Storm, F. Kiessling, T. Lammers, Sonoporation enhances liposome accumulation and penetration in tumors with low EPR, J. Control. Release 231 (2016) 77–85.
[75] J. Huang, K. Pu, Near-infrared fluorescent probes for imaging and diagnosis of nephro-urological diseases, Chem. Sci. 12 (2021) 3379–3392.
[76] A. Hoffman, R. Atreya, T. Rath, M.F. Neurath, Use of Fluorescent Dyes in Endoscopy and Diagnostic Investigation, Visc Med 36 (2020) 95–103.
[77] A. Goyal, New Technologies for Sentinel Lymph Node Detection, Breast Care (Basel) 13 (2018) 349–353.
[78] S. Moestue, P. Nunez, A. Healey, R. Bjerke, B. Indrevoll, T. Skotland, S.O. Hustvedt, Whole-body section fluorescence imaging–a novel method for tissue distribution studies of fluorescent substances, Contrast Media Mol. Imaging 4 (2009) 73–80.
[79] T. Yu, J. Zhu, D. Li, D. Zhu, Physical and chemical mechanisms of tissue optical clearing, iScience 24 (2021) 102178.
[80] T. Skotland, S.O. Hustvedt, I. Oulie, P.B. Jacobsen, G.A. Friisk, A.S. Langoy, S. Uran, J. Sandosham, A. Cuthbertson, K.G. Toft, Nc100668, a new tracer for imaging of venous thromboembolism: disposition and metabolism in rats, Drug Metab. Dispos. 34 (2006) 111–120.
[81] D.P. Bishop, N. Cole, T. Zhang, P.A. Doble, D.J. Hare, A guide to integrating immunohistochemistry and chemical imaging, Chem. Soc. Rev. 47 (2018) 3770–3787.
[82] Y. Komohara, Y. Fujiwara, K. Ohnishi, M. Takeya, Tumor-associated macrophages: Potential therapeutic targets for anti-cancer therapy, Adv. Drug Deliv. Rev. 99 (2016) 180–185.
[83] S. Ebrahim, R. Weigert, Intravital microscopy in mammalian multicellular organisms, Curr. Opin. Cell Biol. 59 (2019) 97–103.
[84] T.S. Haddad, P. Friedl, N. Farahani, D. Treanor, I. Zlobec, I. Nagtegaal, Tutorial: methods for three-dimensional visualization of archival tissue material, Nat. Protoc. 16 (2021) 4945–4962.
[85] G. Sighinolfi, S. Clark, L. Blanc, D. Cota, B. Rhourri-Frih, Mass spectrometry imaging of mice brain lipid profile changes over time under high fat diet, Sci. Rep. 11 (2021) 19664.
[86] A.R. Buchberger, K. DeLaney, J. Johnson, L. Li, Mass Spectrometry Imaging: A Review of Emerging Advancements and Future Insights, Anal. Chem. 90 (2018) 240–265.
[87] M.M. Nabi, M.A. Mamun, A. Islam, M.M. Hasan, A.S.M. Waliullah, Z. Tamannaa, T. Sato, T. Kahyo, M. Setou, Mass spectrometry in the lipid study of cancer, Expert Rev Proteomics 18 (2021) 201–219.
[88] E.G. Solon, A. Schweitzer, M. Stoeckli, B. Prideaux, Autoradiography, MALDI-MS, and SIMS-MS imaging in pharmaceutical discovery and development, AAPS J. 12 (2010) 11–26.
[89] C. Giesen, H.A. Wang, D. Schapiro, N. Zivanovic, A. Jacobs, B. Hattendorf, P.J. Schuffler, D. Grolimund, J.M. Buhmann, S. Brandt, Z. Varga, P.J. Wild, D. Gunther, B. Bodenmiller, Highly multiplexed imaging of tumor tissues with subcellular resolution by mass cytometry, Nat. Methods 11 (2014) 417–422.

[90] A. Adan, G. Alizada, Y. Kiraz, Y. Baran, A. Nalbant, Flow cytometry: basic principles and applications, Crit. Rev. Biotechnol. 37 (2017) 163–176.
[91] A. Reichard, K. Asosingh, Best Practices for Preparing a Single Cell Suspension from Solid Tissues for Flow Cytometry, Cytometry A 95 (2019) 219–226.
[92] M.H. Spitzer, G.P. Nolan, Mass Cytometry: Single Cells, Many Features, Cell 165 (2016) 780–791.
[93] H.J. Byrne, F. Bonnier, E. Efeoglu, C. Moore, J. McIntyre, In vitro Label Free Raman Microspectroscopic Analysis to Monitor the Uptake, Fate and Impacts of Nanoparticle Based Materials, Front. Bioeng. Biotechnol 8 (2020) 544311.
[94] A.D. Pandya, A. Overbye, P. Sahariah, V.S. Gaware, H. Hogset, M. Masson, A. Hogset, G.M. Maelandsmo, T. Skotland, K. Sandvig, T.G. Iversen, Drug-Loaded Photosensitizer-Chitosan Nanoparticles for Combinatorial Chemo- and Photodynamic-Therapy of Cancer, Biomacromolecules 21 (2020) 1489–1498.
[95] P. Paramasivam, C. Franke, M. Stoter, A. Hoijer, S. Bartesaghi, A. Sabirsh, L. Lindfors, M.Y. Arteta, A. Dahlen, A. Bak, S. Andersson, Y. Kalaidzidis, M. Bickle, M. Zerial, Endosomal escape of delivered mRNA from endosomal recycling tubules visualized at the nanoscale, J. Cell Biol. 221 (2021) e202110137.
[96] G. Di Rocco, S. Baldari, G. Toietta, Towards Therapeutic Delivery of Extracellular Vesicles: Strategies for In Vivo Tracking and Biodistribution Analysis, Stem Cells Int. 2016 (2016) 5029619.
[97] Y.W. Yi, J.H. Lee, S.Y. Kim, C.G. Pack, D.H. Ha, S.R. Park, J. Youn, B.S. Cho, Advances in Analysis of Biodistribution of Exosomes by Molecular Imaging, Int. J. Mol. Sci. 21 (2020) 665.
[98] M. Kang, V. Jordan, C. Blenkiron, L.W. Chamley, Biodistribution of extracellular vesicles following administration into animals: A systematic review, J. Extracell Vesicles 10 (2021) e12085.
[99] T. Smyth, M. Kullberg, N. Malik, P. Smith-Jones, M.W. Graner, T.J. Anchordoquy, Biodistribution and delivery efficiency of unmodified tumor-derived exosomes, J. Control. Release 199 (2015) 145–155.
[100] F.N. Faruqu, J.T. Wang, L. Xu, L. McNickle, E.M. Chong, A. Walters, M. Gurney, A. Clayton, L.A. Smyth, R. Hider, J. Sosabowski, K.T. Al-Jamal, Membrane Radiolabelling of Exosomes for Comparative Biodistribution Analysis in Immunocompetent and Immunodeficient Mice - A Novel and Universal Approach, Theranostics 9 (2019) 1666–1682.
[101] D.W. Hwang, H. Choi, S.C. Jang, M.Y. Yoo, J.Y. Park, N.E. Choi, H.J. Oh, S. Ha, Y.S. Lee, J.M. Jeong, Y.S. Gho, D.S. Lee, Noninvasive imaging of radiolabeled exosome-mimetic nanovesicle using (99m)Tc-HMPAO, Sci. Rep. 5 (2015) 15636.
[102] P. Gangadaran, C.M. Hong, B.C. Ahn, An Update on in Vivo Imaging of Extracellular Vesicles as Drug Delivery Vehicles, Front. Pharmacol. 9 (2018) 169.
[103] H. Lee, J. Zheng, D. Gaddy, K.D. Orcutt, S. Leonard, E. Geretti, J. Hesterman, C. Harwell, J. Hoppin, D.A. Jaffray, T. Wickham, B.S. Hendriks, D. Kirpotin, A gradient-loadable (64)Cu-chelator for quantifying tumor deposition kinetics of nanoliposomal therapeutics by positron emission tomography, Nanomedicine 11 (2015) 155–165.
[104] S. Shi, T. Li, X. Wen, S.Y. Wu, C. Xiong, J. Zhao, V.R. Lincha, D.S. Chow, Y. Liu, A. K. Sood, C. Li, Copper-64 Labeled PEGylated Exosomes for In Vivo Positron Emission Tomography and Enhanced Tumor Retention, Bioconjug. Chem. 30 (2019) 2675–2683.
[105] Z. Varga, I. Gyurko, K. Paloczi, E.I. Buzas, I. Horvath, N. Hegedus, D. Mathe, K. Szigeti, Radiolabeling of Extracellular Vesicles with (99m)Tc for Quantitative In Vivo Imaging Studies, Cancer Biother. Radiopharm. 31 (2016) 168–173.
[106] Z. Varga, I.C. Szigyártó, I. Gyurkó, R. Dóczi, I. Horváth, D. Máthé, K. Szigeti, Radiolabeling and Quantitative In Vivo SPECT/CT Imaging Study of Liposomes Using the Novel Iminothiolane-(99m)Tc-Tricarbonyl Complex, Contrast Media Mol. Imaging 2017 (2017) 4693417.
[107] P. Gangadaran, B.C. Ahn, Extracellular Vesicle- and Extracellular Vesicle Mimetics-Based Drug Delivery Systems: New Perspectives, Challenges, and Clinical Developments, Pharmaceutics 12 (2020) 442.
[108] C. Perez-Campana, V. Gomez-Vallejo, M. Puigivila, A. Martin, T. Calvo-Fernandez, S.E. Moya, R.F. Ziolo, T. Reese, J. Llop, Biodistribution of different sized nanoparticles assessed by positron emission tomography: a general strategy for direct activation of metal oxide particles, ACS Nano 7 (2013) 3498–3505.
[109] R. Munter, K. Kristensen, D. Pedersbaek, J.B. Larsen, J.B. Simonsen, T.L. Andresen, Dissociation of fluorescently labeled lipids from liposomes in biological environments challenges the interpretation of uptake studies, Nanoscale 10 (2018) 22720–22724.
[110] A.S. Klymchenko, F. Liu, M. Collot, N. Anton, Dye-Loaded Nanoemulsions: Biomimetic Fluorescent Nanocarriers for Bioimaging and Nanomedicine, Adv. Healthc. Mater. 10 (2021) e2001289.
[111] M. Keyaerts, V. Caveliers, T. Lahoutte, Bioluminescence imaging: looking beyond the light, Trends Mol. Med. 18 (2012) 164–172.
[112] E. Lazaro-Ibanez, F.N. Faruqu, A.F. Saleh, A.M. Silva, J. Tzu-Wen Wang, J. Rak, K.T. Al-Jamal, N. Dekker, Selection of Fluorescent, Bioluminescent, and Radioactive Tracers to Accurately Reflect Extracellular Vesicle Biodistribution in Vivo, ACS Nano 15 (2021) 3212–3227.
[113] N.M. Rofsky, A.D. Sherry, R.E. Lenkinski, Nephrogenic systemic fibrosis: a chemical perspective, Radiology 247 (2008) 608–612.
[114] T.J. Clough, L. Jiang, K.L. Wong, N.J. Long, Ligand design strategies to increase stability of gadolinium-based magnetic resonance imaging contrast agents, Nat. Commun. 10 (2019) 1420.
[115] Y. Takahashi, M. Nishikawa, H. Shinotsuka, Y. Matsui, S. Ohara, T. Imai, Y. Takakura, Visualization and in vivo tracking of the exosomes of murine melanoma B16-BL6 cells in mice after intravenous injection, J. Biotechnol. 165 (2013) 77–84.
[116] B. Davies, T. Morris, Physiological parameters in laboratory animals and humans, Pharm. Res. 10 (1993) 1093–1095.
[117] A.D. Pandya, T.G. Iversen, S. Moestue, M.T. Grinde, Y. Morch, S. Snipstad, A.K. O. Aslund, G.F. Oy, W. Kildal, O. Engebraten, K. Sandvig, T. Skotland, G.M. Maelandsmo, Biodistribution of Poly(alkyl cyanoacrylate) Nanoparticles in Mice and Effect on Tumor Infiltration of Macrophages into a Patient-Derived Breast Cancer Xenograft, Nanomaterials (Basel) 11 (2021) 1140.
[118] A. Bose, I. Thomas, K.G.E. Abraham, Fluorescence spectroscopy and its applications: A Review, International Journal of Advances in Pharmaceutical Analysis, 8 (2018) 01-08.
[119] J.B. Simonsen, E.B. Kromann, Pitfalls and opportunities in quantitative fluorescence-based nanomedicine studies - A commentary, J. Control. Release 335 (2021) 660–667.
[120] S. Skoczen, S.E. McNeil, S.T. Stern, Stable isotope method to measure drug release from nanomedicines, J. Control. Release 220 (2015) 169–174.
[121] The 30-minute guide to ICP-MS, 2010.
[122] S.C. Wilschefski, M.R. Baxter, Inductively Coupled Plasma Mass Spectrometry: Introduction to Analytical Aspects, Clin. Biochem. Rev. 40 (2019) 115–133.
[123] K. Glunde, Z.M. Bhujwalla, Metabolic tumor imaging using magnetic resonance spectroscopy, Semin. Oncol. 38 (2011) 26–41.
[124] K.M. Tsoi, S.A. MacParland, X.Z. Ma, V.N. Spetzler, J. Echeverri, B. Ouyang, S.M. Fadel, E.A. Sykes, N. Goldaracena, J.M. Kaths, J.B. Conneely, B.A. Alman, M. Selzner, M.A. Ostrowski, O.A. Adeyi, A. Zilman, I.D. McGilvray, W.C. Chan, Mechanism of hard-nanomaterial clearance by the liver, Nat. Mater. 15 (2016) 1212–1221.
[125] M. Cataldi, C. Vigliotti, T. Mosca, M. Cammarota, D. Capone, Emerging Role of the Spleen in the Pharmacokinetics of Monoclonal Antibodies, Nanoparticles and Exosomes, Int. J. Mol. Sci. 18 (2017) 1249.
[126] H. Pertoft, B. Smedsrod, Separation and characterization of liver cells, in: T.G. Pretlow, T.P. Pretolw (Eds.), Cell Separation: Methods and Selected Applications, Academic Press, 1987, pp. 1–24.
[127] Y.N. Zhang, W. Poon, A.J. Tavares, I.D. McGilvray, W.C.W. Chan, Nanoparticle-liver interactions: Cellular uptake and hepatobiliary elimination, J. Control. Release 240 (2016) 332–348.
[128] M.P. Chao, I.L. Weissman, R. Majeti, The CD47-SIRPalpha pathway in cancer immune evasion and potential therapeutic implications, Curr. Opin. Immunol. 24 (2012) 225–232.
[129] S. Kamerkar, V.S. LeBleu, H. Sugimoto, S. Yang, C.F. Ruivo, S.A. Melo, J.J. Lee, R. Kalluri, Exosomes facilitate therapeutic targeting of oncogenic KRAS in pancreatic cancer, Nature 546 (2017) 498–503.
[130] G.K. Atkin-Smith, Phagocytic clearance of apoptotic, necrotic, necroptotic and pyroptotic cells, Biochem. Soc. Trans. 49 (2021) 793–804.
[131] M. Hadjidemetriou, Z. Al-Ahmady, M. Mazza, R.F. Collins, K. Dawson, K. Kostarelos, In Vivo Biomolecule Corona around Blood-Circulating, Clinically Used and Antibody-Targeted Lipid Bilayer Nanoscale Vesicles, ACS Nano 9 (2015) 8142–8156.
[132] R.T. Proffitt, L.E. Williams, C.A. Presant, G.W. Tin, J.A. Uliana, R.C. Gamble, J.D. Baldeschwieler, Liposomal blockade of the reticuloendothelial system: improved tumor imaging with small unilamellar vesicles, Science 220 (1983) 502–505.
[133] T. Liu, H. Choi, R. Zhou, I.W. Chen, RES blockade: A strategy for boosting efficiency of nanoparticle drug, Nano Today 10 (2015) 11–21.
[134] B. Ouyang, W. Poon, Y.N. Zhang, Z.P. Lin, B.R. Kingston, A.J. Tavares, Y. Zhang, J. Chen, M.S. Valic, A.M. Syed, P. MacMillan, J. Couture-Senecal, G. Zheng, W.C. W. Chan, The dose threshold for nanoparticle tumour delivery, Nat. Mater. 19 (2020) 1362–1371.
[135] K. Nemeth, Z. Varga, D. Lenzinger, T. Visnovitz, A. Koncz, N. Hegedus, A. Kittel, D. Mathe, K. Szigeti, P. Lorincz, C. O'Neill, R. Dwyer, Z. Liu, E.I. Buzas, V. Tamasi, Extracellular vesicle release and uptake by the liver under normo- and hyperlipidemia, Cell. Mol. Life Sci. 78 (2021) 7589–7604.
[136] M.M. Swindle, A. Makin, A.J. Herron, F.J. Clubb Jr., K.S. Frazier, Swine as models in biomedical research and toxicology testing, Vet. Pathol. 49 (2012) 344–356.
[137] T. Skotland, Injection of nanoparticles into cloven-hoof animals: Asking for trouble, Theranostics 7 (2017) 4877–4878.
[138] G.C. Winkler, Pulmonary intravascular macrophages in domestic animal species: review of structural and functional properties, Am. J. Anat 181 (1988) 217–234.
[139] J.D. Brain, R.M. Molina, M.M. DeCamp, A.E. Warner, Pulmonary intravascular macrophages: their contribution to the mononuclear phagocyte system in 13 species, Am. J. Physiol. 276 (1999) L146–L154.
[140] S. Prabhakar, Translational research challenges: finding the right animal models, J. Invest. Med. 60 (2012) 1141–1146.
[141] K. Wartha, F. Herting, M. Hasmann, Fit-for purpose use of mouse models to improve predictivity of cancer therapeutics evaluation, Pharmacol. Ther. 142 (2014) 351–361.
[142] N. Gengenbacher, M. Singhal, H.G. Augustin, Preclinical mouse solid tumour models: status quo, challenges and perspectives, Nat. Rev. Cancer 17 (2017) 751–765.
[143] A. Gabizon, M. Chemla, D. Tzemach, A.T. Horowitz, D. Goren, Liposome longevity and stability in circulation: effects on the in vivo delivery to tumors and therapeutic efficacy of encapsulated anthracyclines, J. Drug Target. 3 (1996) 391–398.
[144] F. Kiessling, M.E. Mertens, J. Grimm, T. Lammers, Nanoparticles for imaging: top or flop?, Radiology 273 (2014) 10–28